ABSTRACT

DISCRETE DYNAMICAL POPULATION MODELS: HIGHER DIMENSIONAL PIONEER-CLIMAX MODELS

by
Yogesh Joshi

There are many population models in the literature for both continuous and discrete systems. This investigation begins with a general discrete model that subsumes almost all of the discrete population models currently in use. Some results related to the existence of fixed points are proved. Before launching into a mathematical analysis of the primary discrete dynamical model investigated in this dissertation, the basic elements of the model - pioneer and climax species - are described and discussed from an ecological as well as a dynamical systems perspective. An attempt is made to explain why the chosen hierarchical form of the model to explain why the chosen hierarchical form of the model can be expected to follow the real-world evolution of pioneer-climax species. Following the discussion of the discrete dynamical model from the applications viewpoint, an extensive dynamical systems investigation is conducted using analytical and simulation tools. Fixed and periodic points are found and their stability is investigated. Sufficient conditions for the existence and stability of n -cycles are proved and illustrated for several values of n. For eample, the existence of a stable, attracting 3-cycle is proved for a certain range of parameters for an all-pioneer model. It is also observed that the hierarchical system has a predisposition to period-doubling behavior.

Bifurcations of the hierarchical model are studied in considerable depth. It is proved, for example, that the model cannot exhibit a Hopf Bifurcation. However, in a series of theorems, it is shown that the system can exhibit a very rich array of flip (period-doubling) bifurcations, which are of codimension one, two or three. A key to proving this result is that the hierarchical nature of the system makes it

essentially equivalent to a sequence of one-dimensional systems when it comes to several properties of the dynamics. This hierarchical principle is then used to prove chaos for the system in the limit of a period-doubling cascade, and also in terms of shift map behavior on an invariant two-component Cantor set for systems containing a climax component. Bifurcation diagrams and Lyapunov diagrams are computed to further illustrate the chaotic dynamics. Finally, the concept of a 3-dimensional horseshoe type map is also used to prove the existence of chaos in an approximate graphical manner.

DISCRETE DYNAMICAL POPULATION MODELS: HIGHER DIMENSIONAL PIONEER-CLIMAX MODELS

by
Yogesh Joshi

A Dissertation
Submitted to the Faculty of
New Jersey Institute of Technology
Rutgers, The State University of New Jersey – Newark
in Partial Fulfillment of the Requirements for the Degree of
Doctor of Philosophy in Mathematical Sciences

Department of Mathematical Sciences, NJIT
Department of Mathematics and Computer Science, Rutgers-Newark

May 2009

APPROVAL PAGE

DISCRETE DYNAMICAL POPULATION MODELS: HIGHER DIMENSIONAL PIONEER-CLIMAX MODELS

Yogesh Joshi

4/24/09

Dr. Denis L. Blackmore, Dissertation Advisor — Date
Full Professor, Department of Mathematical Sciences, NJIT

4/24/09

Dr. Roy H. Goodman, Committee Member — Date
Associate Professor, Department of Mathematical Sciences, NJIT

4/24/2009

Dr. Frank C. Hoppensteadt, Committee Member — Date
Research Professor, Department of Mathematical Sciences, NYU and
Counselor to the Provost, NYU

04/24/09

Dr. Horacio G. Rotstein, Committee Member — Date
Assistant Professor, Department of Mathematical Sciences, NJIT

04/24/09

Dr. Gareth J. Russell, Committee Member — Date
Assistant Professor, Department of Biological Sciences, NJIT and
Federated Department of Biological Sciences, NJIT and Rutgers-Newark

BIOGRAPHICAL SKETCH

Author: Yogesh Joshi

Degree: Doctor of Philosophy

Date: May 2009

Date of Birth:

Place of Birth:

Undergraduate and Graduate Education:

- Doctor of Philosophy in Mathematical Sciences,
  New Jersey Institute of Technology, Newark, NJ, 2009
- Master of Science in Applied Mathematics,
  New Jersey Institute of Technology, Newark, NJ, 2009
- Master of Science in Mathematics,
  Indian Institute of Technology, Delhi, India, 2003
- Bachelor of Science in Mathematics,
  Delhi University, Delhi, India, 2001

Major: Mathematical Sciences

Presentations and Publications:

Y. Joshi and D. Blackmore, "Bifurcation and chaos in discrete 3D pioneer-climax models," (in preparation).

Y. Joshi and D. Blackmore, "Discrete Dynamical Population Models: Higher Dimensional Pioneer Climax Models," *The Dana Knox Research Showcase*, NJIT, Newark, NJ, April 8, 2009.

Y. Joshi, A. Joshi, G. Genovese, etc., "Quantifying normal variation in ECGs", *Industrial Mathematical and Statistical Modeling Workshop for Graduate Students*, NC State University, Raleigh, NC, July 21-29, 2008.

Y. Joshi, F. Oloude, N. Krislock, etc., "Supply Chain Optimization for the North American Operations of the Evraz Group", *The PIMS Industrial Problem Solving Workshop and Graduate Industrial Mathematics Modelling Camp*, University of Regina, Regina, Canada, June 9-21, 2008.

Y. Joshi and D. Blackmore, "Dynamics of Discrete Population Models: Higher Dimensional Pioneer Climax Models," *Frontiers in Applied and Computational Mathematics*, Department of Mathematical Sciences, NJIT, May 19-21, 2008.

Y. Joshi and D. Blackmore, "Dynamics of Discrete Population Models: Higher Dimensional Pioneer Climax Models," *Graduate Student Research Day*, NJIT, Newark, NJ, Nov 14, 2007.

Y. Joshi, K. Chen, S. H. Rua, etc., "Analyzing Papilloma Data in Mice", *Industrial Mathematical and Statistical Modeling Workshop for Graduate Students*, NC State University, Raleigh, NC, July 23-31, 2007.

Y. Joshi, D. A. Edwards, C. Breward etc., "Characterization of Molecular Diffusion in the Lens Capsule", *The Annual Workshop on Mathematical Problems in Industry*, University of Delaware, Newark, DE, June 11-15, 2007.

Y. Joshi, D. Boy, K. Newhall etc., "Brownian Chain Evolution: A Propulsion Mechanism?", *The Annual Graduate Student Mathematical Modeling Camp*, Rensselaer Polytechnic Institute, Troy, NY, June 5-8, 2007.

Y. Joshi and D. Blackmore, "Discrete Pioneer-Climax Dynamics: Preliminary Report," *Frontiers in Applied and Computational Mathematics*, Department of Mathematical Sciences, NJIT, May 14-16, 2007.

To my loving parents and sisters.

ACKNOWLEDGMENT

First, I thank my advisor Dr. Denis L. Blackmore for his continuous support and encouragement during the course of my writing this dissertation. I could have not wished for a better or friendlier supervisor. My sincere thanks go to my committee members Dr. Horacio G. Rotstein, Dr. Roy H. Goodman, Dr. Gareth J. Russell and Dr. Frank C. Hoppensteadt. My advisor and committee members guided me through the dissertation process, never accepting less than my best efforts. They meticulously read the entire draft, and their productive criticism, suggestions and questions helped to sharpen and strength the analysis and arguments presented in the study and thus helped in making it much better.

Next, I would like to thank the Department of Mathematical Sciences for providing me with the financial support right from my first day at NJIT. I would like to thank Dr. Daljit S. Ahluwalia and the Selection Committee members for giving me a chance to pursue my Ph. D. at NJIT. I would like to thank and acknowledge the help which I received from various staff members of the Math Department at different stages of my stay at NJIT. In particular, Mrs. Padma Gulati and Susan Sutton helped me on many occasions. Thanks a lot.

Next, my thanks go to my fellow graduate students in the Mathematical Sciences Department; in particular, Anisha Banerjee, Lakshmi Chandrasekaran, Kamyar Malakuti, and Myongkeun Oh. I would also like to thank Arnaud Goullet with whom I had many fruitful conservations related to my dissertation writing and research. Special thanks go to Manmeet Kaur for the help she provided to me during my stay at NJIT. I would also like to thank my friend Pankaj Gupta for all his help.

Finally, I would like to thank my family members. I would like to thank my parents BalKrishan Joshi and Rajeshwari Joshi who have played a pivotal role in my life and in making me stand where I am now, and also my elder sister Laxmi Bhandari

and younger sister Chetna Joshi for their love and affection towards me. I would also like to thank my brother-in-law Dr. Neetesh Bhandari for his encouragement and guidance at various stages of my Ph.D. My nephews Devang Bhandari and Aditya Bhandari (Adi) also deserve thanks. Last, but not the least, I thank God for giving me this life where many dream of but few attain the Ph.D. degree. Thank you God for giving me the strength to reach this goal.

Thank you all!!

TABLE OF CONTENTS

LIST OF FIGURES

Figure **Page**

LIST OF FIGURES
(Continued)

Figure **Page**

CHAPTER 1

BACKGROUND

Population modeling has been a constant and active research area for both dynamical analysts and ecologists. It began with the very simple 1-D Logistic model proposed by the Belgian Mathematician Pierre Verhulst [48, 49]. Since then it has evolved manifold times. Population modeling was not single-handedly developed by applied mathematicians; many ecologists also played a part in developing this field. Most of the population models available in the literature were developed for some particular types of species and low dimensions (i.e., a small number of different species). But they can be extended to higher dimensions and studied from a dynamical behavior point of view. Here we start with an effort to combine all the available models to make a general model that subsumes most of those in current use.

There are many population models (both continuous and discrete) that have been almost completely analyzed. These inspired us to begin with a general population model, which includes most of the popular discrete models. First, we list some well-known models

1. **A general predator-prey model (Werner Krabs):** Consider n populations $X_i;\ i = 1,\ 2,\ 3, \ldots,\ n$ of animals or plants that are living in mutual predator-prey relations or pairwise neutral to each other. Let $X_i(t)$ denote the total members of the i^{th} population and $x_i(t) = \frac{X_i}{\sum X_i}$, be the corresponding density at time t. This model has the form [24]

$$\dot{x_i}(t) = (c_i + \sum_{j=1}^{n} c_{ij} x_j(t)) x_i(t),\ i = 1,\ 2,\ 3,\ \ldots,\ n$$

where

$$c_{ii} \leq 0 \text{ for } i = 1,\ 2,\ 3, \ldots,\ n$$

and for $i \neq j$,

$$c_{ij} > 0, \text{ if } X_i \text{ is a predator and} X_j \text{ is a prey,}$$
$$c_{ij} < 0, \text{ if } X_i \text{ is a prey and } X_j \text{ is a predator,}$$
$$c_{ij} = 0, \text{ if } X_i,\ X_j \text{ are neutral to each other.}$$

This is a generalization of the Lotka-Volterra model [24].

Next we have a discrete version of the above model for $n = 2$, obtained using a forward difference approach.

Let $h > 0$ be step size and replacing $\dot{x_1}(t),\ \dot{x_2}(t)$ respectively by

$$\begin{aligned} \dot{x_1}(t) &= \frac{x_1(t+h) - x_1(t)}{h} \\ \dot{x_2}(t) &= \frac{x_2(t+h) - x_2(t)}{h} \end{aligned} \tag{1.1}$$

we get the following model

$$\begin{aligned} x_1(t+h) &= x_1(t) + h(c_1 + c_{11}x_1(t) + c_{12}x_2(t))x_1(t) \\ x_2(t+h) &= x_2(t) + h(c_2 + c_{21}x_1(t) + c_{22}x_2(t))x_2(t) \end{aligned} \tag{1.2}$$

2. **LPA model (J M Cushing):** It is the nonlinear (Leslie) matrix model of the form [7]:

$$\begin{aligned} L(t+1) &= bA(t)e^{\frac{-C_{el}L(t)}{V} - \frac{C_{ea}A(t)}{V}} \\ P(t+1) &= (1-\mu_l)L(t) \\ A(t+1) &= P(t)e^{(\frac{-C_{pa}A(t)}{V})} + A(t)(1-\mu_a) \end{aligned} \tag{1.3}$$

where $L(t),\ P(t),\ A(t)$ denote the numbers of individuals at time t present in the larval, pupal and adult states, respectively, of the three life cycles of genus

Tribolium (flour beetles). In fact this model can be used for any species which has three life cycle stages. Here

$$V \equiv \text{habitat size}$$

$$b(>0) = \text{is the inherent per adult recruitment of larvae.}$$

μ_l, μ_a satisfy $0 < \mu_l < 1$, $0 < \mu_a \leq 1$ and represent death rates (the fraction of the larvae and adult stages that die each unit of time). The coefficients C_{el}, C_{ea}, C_{pa} account for the cannibalistic encounters and are called "cannibalism coefficients ".

3. **The Leslie-Gower Model** [8]

$$x_{t+1} = b_1 \frac{x_t}{1 + c_{11}x_t + c_{12}y_t}$$
$$y_{t+1} = b_2 \frac{y_t}{1 + c_{21}x_t + c_{22}y_t}$$

where, $c_{ii} > 0$, $b_i > 0$.

4. **Ricker Competition Model** [8]

$$x_{t+1} = b_1 x_t e^{(-c_{11}x_t - c_{12}y_t)}$$
$$y_{t+1} = b_2 y_t e^{(-c_{21}x_t - c_{22}y_t)}$$

where, $b_i > 0$, $c_{ii} > 0$.

1.1 Ecological Studies

Pioneer-Climax species, which usually refer to types of flora, have been studied for many years, by both ecologists and applied mathematicians and more recently have been extensively investigated using a variety of dynamical systems models, most of which have been limited to two-dimensional (two species) models. Many experimental

studies (field work) have also been conducted, with [22, 34, 35, 44] being some of the more recent ones. In [22], Jegan, Ramesh and Muthuchelian showed that pioneer species need light for regeneration and resprouting which are important processes that allow plant species to remain viable in an ecosystem, but which climax species do not require. They evolve in an environment that is made easy to grow and thrive in by their predecessors. Jegan et al. classified their results based on forest openings (closed, small gap and large gap) which played a pivotal role in the study. Raaimakers et al. [34] investigated whether low phosphorous (P) availability limits the process of photosynthesis more than nitrogen (N) does in tree species in Guyana where the soil quality is acidic. The experiment was carried on nine pioneer and climax tree species. They also studied the relationship between leaf P and N content with photosynthetic capacity. They found at similar P and N content, pioneer species have a higher photosynthetic capacity than the climax species in a range of light climates. Photosynthetic characteristics and pattern of biomass accumulation in seedlings of pioneer and climax tree species from Brazil were studied by Silvestrini et al. [44]. The seedlings were grown for four months under low light (5% to 8% sunlight) and high light (100% sunlight). Both species exhibited characteristics that favor growth under conditions that resemble their natural microenvironments. They also found that the climax species grow under high light, which is not observed normally in climax species. They proposed to explain this behavior using the spatio-temporal light regime of the forest. In [25], Kuijk developed and used a model in Vietnam for forest regeneration and restoration. The model evaluates shoot height and plant architecture, biomass allocation patterns and leaf physiology in terms of light capture and photosynthetic gains. Kuijk's model proved to be quite successful when applied to grasslands. Forest regeneration is a successional process where old trees (pioneers) are replaced by the new ones (climax) and a structural change in the forest canopy occurs.

1.2 Mathematical Modeling and Analysis

A three-dimensional difference equation model called the "LPA model" was presented in [7] by Cushing and a detailed study was conducted. Many dynamical results for the model - including the possibility of chaotic behavior - were proved mathematically and demonstrated for the real data obtained from observing Tribolium populations. Franke and Yakubu [11], [12] used a very general 2-species competition model for pioneer-climax interactions with precise mathematical definitions to show the existence of the Pioneer Exclusion Principle, which states that the ultimate dynamical result of an undisturbed system of pioneer species competing with a climax species is exclusion of pioneer species. Hassell and Comins [18] studied a difference equation single and two age-class model for two-species competition. Their model indicated that the populations exhibit damped oscillations, stable cycles and even apparent "chaos" if the competition is sufficiently severe. Selgrade and Namkoong [38] and Sumner [47, 46] showed that certain 2-dimensional (non-hierarchical) differential equation and difference equation pioneer-climax models exhibit stable periodic behavior arising from Hopf Bifurcations. Selgrade and Namkoong [39] analyzed both differential and difference equation models of 2-species interacting pioneer-climax populations. The asymptotic behavior of these model was discussed, and the occurrence of strange attractors was observed. Selgrade and Roberds [40] showed the existence of Hopf bifurcations for deterministic models of the interaction of pioneer and climax populations. In another study Selgrade and Roberds [42] derived conditions for dynamical pioneer-climax models which guaranteed an equilibrium loses stability via period-doubling bifurcation. They also modified and studied the model with a constant term representing stocking or harvesting of the pioneer population and derived another set of conditions which reverses the bifurcation and restabilizes the equilibrium.

1.3 Research Innovations

In this work we will concentrate mainly on a three-dimensional pioneer-climax model, where there has been comparatively little work done from the dynamical systems viewpoint. More specifically, the focus is on three-dimensional hierarchical models, which have proved to be reasonably reliable predictors of pioneer-climax system evolution. We shall describe an extensive theoretical and computational investigation of discrete three-dimensional hierarchical pioneer-climax models, including an analysis of fixed and periodic points, bifurcations, and chaotic regimes, which are as far as possible framed in an applied ecological context. Among our contributions are novel results for discrete dynamical three-dimensional pioneer-climax models on flip-bifurcation cascades, stable and unstable periodic orbits, and the existence of chaotic regimes that appear to be associated with strange attractors.

This dissertation is organized as follows: In Chapter 2, we briefly study a very general population dynamical model and perform a brief analysis of its fixed point. Then in Chapter 3, we introduce pioneer and climax species and the discrete mathematical equations that we shall use to model their behavior. We then focus on a three-dimensional pioneer-climax model and in particular an hierarchical model. In Chapter 4, a local stability analysis is performed on the model. In Chapter 5, various aspects of periodic behavior of the species are analyzed, and in Chapter 6, a rather extensive analysis of bifurcations of the model - especially flip-bifurcations - is undertaken. Finally, several types of chaotic dynamics occurring at various parameter values are analyzed.

CHAPTER 2

A GENERAL DISCRETE DYNAMIC POPULATION MODEL

Before going to our main focus of dynamical analysis of pioneer-climax models, we first present, make some observations and perform fixed point analysis of a very general discrete model, which subsumes all the known models in the literature. As we shall see, without adding more specific details, it is difficult to prove many general results other than fixed point theorems. Of course, fixed points represent stationary states for such models and are therefore very important.

Based on the models in Chapter 1, we present a very general discrete dynamical population model, which can be written in the following way:

$$X_{k+1} = \Phi(X_k), \tag{2.1}$$

$$\text{where } X = (x_1,\ x_2,\ \cdots,\ x_n)^T, \tag{2.2}$$

$$\Phi(X) = (\phi_1(X),\ \phi_2(X),\ \cdots,\ \phi_n(X))^T, \tag{2.3}$$

$$\phi_m(X) = f_m(D_m(X)X) + g_m(\Delta_m(X)X), \tag{2.4}$$

$$f_m(X) = \alpha_m^{(0)} + \alpha_m^{(1)} x_m, \tag{2.5}$$

$$g_m(X) = \frac{P_m(X)}{Q_m(X)}, \tag{2.6}$$

$$P_m(X) = P_m^{(0)} + \sum_{j=1}^{n} P_m^{(j)} x_j + \sum_{1\le i\le j\le n} P_m^{(ij)} x_i x_j, \tag{2.7}$$

$$Q_m(X) = 1 + \sum_{j=1}^{n} q_m^{(j)} x_j + \sum_{1\le i\le j\le n} q_m^{(ij)} x_i x_j, \tag{2.8}$$

where

$$D_m(X) = \begin{bmatrix} e^{-<A_m^{(1)},\ X>} & 0 & 0 & \dots & 0 \\ 0 & e^{-<A_m^{(2)},\ X>} & 0 & \dots & 0 \\ 0 & 0 & e^{-<A_m^{(3)},\ X>} & \dots & 0 \\ \vdots & \vdots & \vdots & \ddots & \vdots \\ 0 & 0 & \dots & 0 & e^{-<A_m^{(n)},\ X>} \end{bmatrix} \tag{2.9}$$

and

$$\Delta_m(X) = \begin{bmatrix} e^{-<B_m^{(1)},\ X>} & 0 & 0 & \dots & 0 \\ 0 & e^{-<B_m^{(2)},\ X>} & 0 & \dots & 0 \\ 0 & 0 & e^{-<B_m^{(3)},\ X>} & \dots & 0 \\ \vdots & \vdots & \vdots & \ddots & \vdots \\ 0 & 0 & \dots & 0 & e^{-<B_m^{(n)},\ X>} \end{bmatrix} \tag{2.10}$$

In our general discrete population model we have:

1. $A_m^{(j)}$, $B_m^{(j)}$, $1 \leq j,\ m \leq n$ are fixed (n-dimensional) vectors having all components non-negative. Note that we will be concentrating on such vectors with non-negative components, and it is convenient to denote the positive orthant of all such vectors as $\mathbf{R}_+^n$.

2. $< V_1,\ V_2 >$, denotes the inner product of two vectors V_1, V_2 which in our case is defined by componentwise multiplication.

In particular a 3-species general population model can be written as:

$$X_{k+1} = \Phi(X_k), \tag{2.11}$$

where

$$X = (x_1,\ x_2,\ x_3)^T, \tag{2.12}$$

$$\Phi(X) = (\phi_1(X),\ \phi_2(X),\ \phi_3(X))^T, \tag{2.13}$$

$$\phi_1(X) = \alpha_1^{(0)} + \alpha_1^{(1)} x_1 e^{-<A_1^{(1)},\, X>}$$

$$+ \frac{P_1^{(0)} + \sum_{j=1}^{3} P_1^{(j)} x_j e^{-<A_1^{(j)},\, X>} + \sum_{1\le i\le j\le 3} P_1^{(ij)} x_i e^{-<A_1^{(i)},\, X>} x_j e^{-<A_1^{(j)},\, X>}}{1 + \sum_{j=1}^{3} q_1^{(j)} x_j e^{-<B_1^{(j)},\, X>} + \sum_{1\le i\le j\le 3} q_1^{(ij)} x_i e^{-<B_1^{(i)},\, X>} x_j e^{-<B_1^{(j)},\, X>}} \tag{2.14}$$

$$\phi_2(X) = \alpha_2^{(0)} + \alpha_2^{(1)} x_2 e^{-<A_2^{(2)},\, X>}$$

$$+ \frac{P_2^{(0)} + \sum_{j=1}^{3} P_2^{(j)} x_j e^{-<A_2^{(j)},\, X>} + \sum_{1\le i\le j\le 3} P_2^{(ij)} x_i e^{-<A_2^{(i)},\, X>} x_j e^{-<A_2^{(j)},\, X>}}{1 + \sum_{j=1}^{3} q_2^{(j)} x_j e^{-<B_2^{(j)},\, X>} + \sum_{1\le i\le j\le 3} q_2^{(ij)} x_i e^{-<B_2^{(i)},\, X>} x_j e^{-<B_2^{(j)},\, X>}} \tag{2.15}$$

$$\phi_3(X) = \alpha_3^{(0)} + \alpha_3^{(1)} x_3 e^{-<A_3^{(3)},\, X>}$$

$$+ \frac{P_3^{(0)} + \sum_{j=1}^{3} P_3^{(j)} x_j e^{-<A_3^{(j)},\, X>} + \sum_{1\le i\le j\le 3} P_3^{(ij)} x_i e^{-<A_3^{(i)},\, X>} x_j e^{-<A_3^{(j)},\, X>}}{1 + \sum_{j=1}^{3} q_3^{(j)} x_j e^{-<B_3^{(j)},\, X>} + \sum_{1\le i\le j\le 3} q_3^{(ij)} x_i e^{-<B_3^{(i)},\, X>} x_j e^{-<B_3^{(j)},\, X>}} \tag{2.16}$$

2.1 Existence of Fixed Points For a General Three Species Model

In the investigation of any dynamical system a primary step is to find fixed or equilibrium points. We proceed to find conditions which guarantee the existence of fixed points, but as the general system tends to be overly cumbersome, we shall confine most of our detailed analysis to the three-dimensional case, noting that our results can be readily extended to the $n-$dimensional case. We will use the celebrated fixed point theorems of Banach and Brouwer for the stated purpose. We begin with Banach's Fixed Point Theorem (also called the Contraction Mapping Principle) to find conditions for a unique fixed point to exist.

Let

$$X = (x_1,\ x_2,\ x_3)^T,\ Y = (y_1,\ y_2,\ y_3)^T \tag{2.17}$$

$$\Phi(X) = (\phi_1(X),\ \phi_2(X),\ \phi_3(X))^T \tag{2.18}$$

$$\Phi(Y) = (\phi_1(Y),\ \phi_2(Y),\ \phi_3(Y))^T \tag{2.19}$$

We need to show, $d(\Phi(X),\ \Phi(Y)) \leq \alpha d(X, Y)$, with $\alpha \in (0, 1)$.

where,

$$d(\Phi(X),\ \Phi(Y)) = \sqrt{(\phi_1(X) - \phi_1(Y))^2 + (\phi_2(X) - \phi_2(Y))^2 + (\phi_3(X) - \phi_3(Y))^2}$$

$$\phi_1(X) = \alpha_1^{(0)} + \alpha_1^{(1)} x_1 e^{-<A_1^{(1)},\ X>}$$

$$+ \frac{P_1^{(0)} + \sum_{j=1}^{3} P_1^{(j)} x_j e^{-<A_1^{(j)},\ X>} + \sum_{1\leq i\leq j\leq 3} P_1^{(ij)} x_i e^{-<A_1^{(i)},\ X>} x_j e^{-<A_1^{(j)},\ X>}}{1 + \sum_{j=1}^{3} q_1^{(j)} x_j e^{-<B_1^{(j)},\ X>} + \sum_{1\leq i\leq j\leq 3} q_1^{(ij)} x_i e^{-<B_1^{(i)},\ X>} x_j e^{-<B_1^{(j)},\ X>}}$$

$$\phi_1(Y) = \alpha_1^{(0)} + \alpha_1^{(1)} y_1 e^{-<A_1^{(1)},\ Y>}$$

$$+ \frac{P_1^{(0)} + \sum_{j=1}^{3} P_1^{(j)} y_j e^{-<A_1^{(j)},\ Y>} + \sum_{1\leq i\leq j\leq 3} P_1^{(ij)} y_i e^{-<A_1^{(i)},\ Y>} y_j e^{-<A_1^{(j)},\ Y>}}{1 + \sum_{j=1}^{3} q_1^{(j)} y_j e^{-<B_1^{(j)},\ Y>} + \sum_{1\leq i\leq j\leq 3} q_1^{(ij)} y_i e^{-<B_1^{(i)},\ Y>} y_j e^{-<B_1^{(j)},\ Y>}}$$

$$\phi_2(X) = \alpha_2^{(0)} + \alpha_2^{(1)} x_2 e^{-<A_2^{(2)},\ X>}$$

$$+ \frac{P_2^{(0)} + \sum_{j=1}^{3} P_2^{(j)} x_j e^{-<A_2^{(j)},\ X>} + \sum_{1\leq i\leq j\leq 3} P_2^{(ij)} x_i e^{-<A_2^{(i)},\ X>} x_j e^{-<A_2^{(j)},\ X>}}{1 + \sum_{j=1}^{3} q_2^{(j)} x_j e^{-<B_2^{(j)},\ X>} + \sum_{1\leq i\leq j\leq 3} q_2^{(ij)} x_i e^{-<B_2^{(i)},\ X>} x_j e^{-<B_2^{(j)},\ X>}}$$

$$\phi_2(Y) = \alpha_2^{(0)} + \alpha_2^{(1)} y_2 e^{-<A_2^{(2)},\ Y>}$$

$$+ \frac{P_2^{(0)} + \sum_{j=1}^{3} P_2^{(j)} y_j e^{-<A_2^{(j)},\ Y>} + \sum_{1\le i\le j\le 3} P_2^{(ij)} y_i e^{-<A_2^{(i)},\ Y>} y_j e^{-<A_2^{(j)},\ Y>}}{1 + \sum_{j=1}^{3} q_2^{(j)} y_j e^{-<B_2^{(j)},\ Y>} + \sum_{1\le i\le j\le 3} q_2^{(ij)} y_i e^{-<B_2^{(i)},\ Y>} y_j e^{-<B_2^{(j)},\ Y>}}$$

$$\phi_3(X) = \alpha_3^{(0)} + \alpha_3^{(1)} x_3 e^{-<A_3^{(2)},\ X>}$$

$$+ \frac{P_3^{(0)} + \sum_{j=1}^{3} P_3^{(j)} x_j e^{-<A_3^{(j)},\ X>} + \sum_{1\le i\le j\le 3} P_3^{(ij)} x_i e^{-<A_3^{(i)},\ X>} x_j e^{-<A_3^{(j)},\ X>}}{1 + \sum_{j=1}^{3} q_3^{(j)} x_j e^{-<B_3^{(j)},\ X>} + \sum_{1\le i\le j\le 3} q_3^{(ij)} x_i e^{-<B_3^{(i)},\ X>} x_j e^{-<B_3^{(j)},\ X>}}$$

$$\phi_3(Y) = \alpha_3^{(0)} + \alpha_3^{(1)} y_3 e^{-<A_3^{(2)},\ Y>}$$

$$+ \frac{P_3^{(0)} + \sum_{j=1}^{3} P_3^{(j)} y_j e^{-<A_3^{(j)},\ Y>} + \sum_{1\le i\le j\le 3} P_3^{(ij)} y_i e^{-<A_3^{(i)},\ Y>} y_j e^{-<A_3^{(j)},\ Y>}}{1 + \sum_{j=1}^{3} q_3^{(j)} y_j e^{-<B_3^{(j)},\ Y>} + \sum_{1\le i\le j\le 3} q_3^{(ij)} y_i e^{-<B_3^{(i)},\ Y>} y_j e^{-<B_3^{(j)},\ Y>}}$$

Before we begin proving a result that employs Banach's Theorem [2] to find a (unique) fixed point, we prove a useful elementary lemma.

Lemma 2.0.1. *If* $\phi(x) = xe^{-Ax}$, $A > 0$, *then* $|\phi(x) - \phi(y)| < |x - y|\ \forall\ x,\ y > 0$.

Proof. By the Mean Value Theorem, we have

$$\phi(x) - \phi(y) = \phi'(\xi)(x - y),$$

for some $\xi > 0$ between x and y.

We need to show that $|\phi'(\xi)| < 1$ for $\xi > 0$. But this follows from elementary calculus, noting that

$$\phi(\xi) = \xi e^{-A\xi}, \quad \phi'(\xi) = e^{-A\xi}(1 - A\xi),$$
$$\phi''(\xi) = -Ae^{-A\xi}(2 - A\xi). \tag{2.20}$$

The second derivative vanishes only at $\xi = 2/A$, and from this it is easy to verify the desired property of the derivative. Hence

$$\begin{aligned} |\phi(x) - \phi(y)| &= |\phi'(\xi)(x-y)| \\ &\leq |\phi'(\xi)||(x-y)| \\ |\phi(x) - \phi(y)| &\leq |(x-y)|, \end{aligned} \tag{2.21}$$

which proves the lemma. □

Now we begin with the analysis.

$$\begin{aligned}
d(\Phi(X),\Phi(Y)) =& ((\alpha_1^{(0)} + \alpha_1^{(1)} x_1 e^{-<A_1^{(1)},\ X>} \\
&+ \frac{P_1^{(0)} + \sum_{j=1}^{3} P_1^{(j)} x_j e^{-<A_1^{(j)},\ X>} + \sum_{1\leq i\leq j\leq 3} P_1^{(ij)} x_i e^{-<A_1^{(i)},\ X>} x_j e^{-<A_1^{(j)},\ X>}}{1 + \sum_{j=1}^{3} q_1^{(j)} x_j e^{-<B_1^{(j)},\ X>} + \sum_{1\leq i\leq j\leq 3} q_1^{(ij)} x_i e^{-<B_1^{(i)},\ X>} x_j e^{-<B_1^{(j)},\ X>}} \\
&- \alpha_1^{(0)} - \alpha_1^{(1)} y_1 e^{-<A_1^{(1)},\ Y>} \\
&- \frac{P_1^{(0)} + \sum_{j=1}^{3} P_1^{(j)} y_j e^{-<A_1^{(j)},\ Y>} + \sum_{1\leq i\leq j\leq 3} P_1^{(ij)} y_i e^{-<A_1^{(i)},\ Y>} y_j e^{-<A_1^{(j)},\ Y>}}{1 + \sum_{j=1}^{3} q_1^{(j)} y_j e^{-<B_1^{(j)},\ Y>} + \sum_{1\leq i\leq j\leq 3} q_1^{(ij)} y_i e^{-<B_1^{(i)},\ Y>} y_j e^{-<B_1^{(j)},\ Y>}})^2 \\
&+ (\alpha_2^{(0)} + \alpha_2^{(1)} x_2 e^{-<A_2^{(1)},\ X>} \\
&+ \frac{P_2^{(0)} + \sum_{j=1}^{3} P_2^{(j)} x_j e^{-<A_2^{(j)},\ X>} + \sum_{1\leq i\leq j\leq 3} P_2^{(ij)} x_i e^{-<A_2^{(i)},\ X>} x_j e^{-<A_2^{(j)},\ X>}}{1 + \sum_{j=1}^{3} q_1^{(j)} x_j e^{-<B_2^{(j)},\ X>} + \sum_{1\leq i\leq j\leq 3} q_2^{(ij)} x_i e^{-<B_2^{(i)},\ X>} x_j e^{-<B_2^{(j)},\ X>}} \\
&- \alpha_2^{(0)} - \alpha_2^{(1)} y_1 e^{-<A_2^{(1)},\ Y>} \\
&- \frac{P_2^{(0)} + \sum_{j=1}^{3} P_2^{(j)} y_j e^{-<A_2^{(j)},\ Y>} + \sum_{1\leq i\leq j\leq 3} P_2^{(ij)} y_i e^{-<A_2^{(i)},\ Y>} y_j e^{-<A_2^{(j)},\ Y>}}{1 + \sum_{j=1}^{3} q_1^{(j)} y_j e^{-<B_2^{(j)},\ Y>} + \sum_{1\leq i\leq j\leq 3} q_2^{(ij)} y_i e^{-<B_2^{(i)},\ Y>} y_j e^{-<B_2^{(j)},\ Y>}})^2 \\
&+ (\alpha_3^{(0)} + \alpha_3^{(1)} x_3 e^{-<A_3^{(1)},\ X>} \\
&+ \frac{P_3^{(0)} + \sum_{j=1}^{3} P_3^{(j)} x_j e^{-<A_3^{(j)},\ X>} + \sum_{1\leq i\leq j\leq 3} P_3^{(ij)} x_i e^{-<A_3^{(i)},\ X>} x_j e^{-<A_3^{(j)},\ X>}}{1 + \sum_{j=1}^{3} q_1^{(j)} x_j e^{-<B_3^{(j)},\ X>} + \sum_{1\leq i\leq j\leq 3} q_3^{(ij)} x_i e^{-<B_3^{(i)},\ X>} x_j e^{-<B_3^{(j)},\ X>}} \\
&- \alpha_3^{(0)} - \alpha_3^{(1)} y_3 e^{-<A_3^{(1)},\ Y>} \\
&- \frac{P_3^{(0)} + \sum_{j=1}^{3} P_3^{(j)} y_j e^{-<A_3^{(j)},\ Y>} + \sum_{1\leq i\leq j\leq 3} P_3^{(ij)} y_i e^{-<A_3^{(i)},\ Y>} y_j e^{-<A_3^{(j)},\ Y>}}{1 + \sum_{j=1}^{3} q_1^{(j)} y_j e^{-<B_3^{(j)},\ Y>} + \sum_{1\leq i\leq j\leq 3} q_3^{(ij)} y_i e^{-<B_3^{(i)},\ Y>} y_j e^{-<B_3^{(j)},\ Y>}})^2)^{1/2}
\end{aligned}$$

We introduce these conditions

$$\sum_{j=1}^{3} q_1^{(j)} > 0, \quad \sum_{1\le i,\ j\le 3} q_1^{(ij)} > 0, \quad \sum_{j=1}^{3} q_2^{(j)} > 0,$$
$$\sum_{1\le i,\ j\le 3} q_2^{(ij)} > 0, \quad \sum_{j=1}^{3} q_3^{(j)} > 0, \quad \sum_{1\le i,\ j\le 3} q_3^{(ij)} > 0$$

and using Lemma 2.0.1 (in the numerator) we get,

$$d(\Phi(X),\Phi(Y)) \le ((\alpha_1^{(1)} + P_1^{(1)})(x_1 - y_1) + P_1^{(2)}(x_2 - y_2) + P_1^{(3)}(x_3 - y_3) + \sum P_1^{(ij)}(x_i x_j - y_i y_j))^2$$

$$+ ((\alpha_2^{(1)} + P_2^{(2)})(x_2 - y_2) + P_2^{(1)}(x_1 - y_1) + P_2^{(3)}(x_3 - y_3) + \sum P_2^{(ij)}(x_i x_j - y_i y_j))^2$$

$$+ ((\alpha_3^{(1)} + P_3^{(3)})(x_1 - y_1) + P_3^{(1)}(x_1 - y_1) + P_3^{(2)}(x_2 - y_2) + \sum P_2^{(ij)}(x_i x_j - y_i y_j))^2)^{1/2}$$

We further apply the constraints:

$$P_1^{(ij)} = 0,\ P_2^{(ij)} = 0,\ P_3^{(ij)} = 0 \text{ for all } i,\ j$$

$$(\alpha_1^{(1)} + P_1^{(1)})P_1^{(2)} < 0,\ (\alpha_1^{(1)} + P_1^{(1)})P_1^{(3)} < 0$$

$$(\alpha_2^{(1)} + P_2^{(2)})P_2^{(1)} < 0,\ (\alpha_2^{(1)} + P_2^{(2)})P_2^{(3)} < 0$$

$$(\alpha_3^{(1)} + P_3^{(3)})P_3^{(1)} < 0,\ (\alpha_3^{(1)} + P_3^{(3)})P_3^{(2)} < 0.$$

These assumptions and constraints to put bounds on the population growth rates. With them, we compute that

$$d(\Phi(X),\Phi(Y)) \le ((\alpha_1^{(1)} + P_1^{(1)})^2(x_1 - y_1)^2 + P_1^{(2)^2}(x_2 - y_2)^2 + P_1^{(3)^2}(x_3 - y_3)^2$$

$$+ (\alpha_2^{(1)} + P_2^{(2)})^2 (x_2 - y_2)^2 + P_2^{(1)^2} (x_1 - y_1)^2 + P_2^{(3)^2} (x_3 - y_3)^2$$

$$+ (\alpha_3^{(1)} + P_3^{(3)})^2 (x_3 - y_3)^2 + P_3^{(1)^2} (x_1 - y_1)^2 + P_3^{(2)^2} (x_2 - y_2)^2)^{1/2}$$

$$d(\Phi(X), \Phi(Y)) \leq (((\alpha_1^{(1)} + P_1^{(1)})^2 + P_2^{(1)^2} + P_3^{(1)^2})(x_1 - y_1)^2$$

$$+ ((\alpha_2^{(1)} + P_2^{(2)})^2 + P_1^{(2)^2} + P_2^{(3)^2})(x_2 - y_2)^2)$$

$$+ ((\alpha_3^{(1)} + P_3^{(3)})^2 + P_1^{(3)^2} + P_2^{(3)^2})(x_3 - y_3)^2)^{1/2}$$

so,

$$d(\Phi(X),\ \Phi(Y)) \leq \alpha d(X,\ Y) \tag{2.22}$$

where, $\alpha = c^2 = \text{Max}\{((\alpha_1^{(1)} + P_1^{(1)})^2 + P_2^{(1)^2} + P_3^{(1)^2}),\ ((\alpha_2^{(1)} + P_2^{(2)})^2 + P_1^{(2)^2} + P_3^{(2)^2}),$
$((\alpha_3^{(1)} + P_3^{(3)})^2 + P_1^{(3)^2} + P_2^{(3)^2})\} < 1$

The above analysis can be readily generalized to our n - species general discrete dynamical model given by (2.1-2.10). Thus we have essentially proved the following result.

Theorem 2.0.2. *The n - species general discrete population model given by (2.1-2.10) has a unique fixed point if following conditions are satisfied:*

i) $\sum_{j=1}^{n} q_l^{(j)} > 0,\ \sum_{1 \leq i,j \leq n} q_l^{(ij)} > 0, \quad l = 1,\ 2,\ 3, \cdots,\ n$

ii) $P_l^{(ij)} = 0,\ (\alpha_l^{(1)} + P_l^{(k)}) P_l^{(k)} < 0,$ *for all* $i,\ j,\ l,\ k = 1,\ 2,\ 3,\ \cdots,\ n,\ k \neq l$

iii) $\alpha = c^2 = Max\{((\alpha_l^{(1)} + P_l^{(k)})^2 + P_l^{(k)^2}),\ l,\ k = 1,\ 2,\ 3,\ \cdots,\ n, k \neq l\} < 1.$

Now we will apply Brouwer's Fixed Point Theorem [19], which states that *every continuous function from a closed unit ball to itself has at least one fixed point*, to our general 3-species discrete population model.

Let

$$X = (x_1,\ x_2,\ x_3)^T, \quad \Phi(X) = (\phi_1(x_1,\ x_2,\ x_3),\ \phi_2(x_1,\ x_2,\ x_3),\ \phi_3(x_1,\ x_2,\ x_3))^T$$

and

$$D^3 = (x_1,\ x_2,\ x_3)^T \in \mathbb{R}^3 : x_1^2 + x_2^2 + x_3^2 \leq 1 \text{ be the closed unit sphere}$$

We need to find the conditions on the parameters so that $\Phi(D) \subset D^3$.

$$\phi_1(X) = \alpha_1^{(0)} + \alpha_1^{(1)} x_1 e^{-<A_1^{(1)},\ X>}$$

$$+ \frac{P_1^{(0)} + \sum_{j=1}^{3} P_1^{(j)} x_j e^{-<A_1^{(j)},\ X>} + \sum_{1\leq i\leq j\leq 3} P_1^{(ij)} x_i e^{-<A_1^{(i)},\ X>} x_j e^{-<A_1^{(j)},\ X>}}{1 + \sum_{j=1}^{3} q_1^{(j)} x_j e^{-<B_1^{(j)},\ X>} + \sum_{1\leq i\leq j\leq 3} q_1^{(ij)} x_i e^{-<B_1^{(i)},\ X>} x_j e^{-<B_1^{(j)},\ X>}}$$

so using the conditions

$$\sum_{j=1}^{3} q_1^{(j)} \geq 0, \qquad \sum_{1\leq i,\ j\leq 3} q_1^{(ij)} \geq 0,$$

we find that

$$\phi_1(X) \leq \alpha_1^{(0)} + \alpha_1^{(1)} x_1 + P_1^{(0)} + \sum_{j=1}^{3} P_1^{(j)} x_j + \sum_{1\leq i\leq j\leq 3} P_1^{(ij)} x_i x_j.$$

Now $x_1^2 + x_2^2 + x_3^2 \leq 1$, so either $x_1 < 1,\ x_2 < 1,\ x_3 < 1$ or $x_1 = 1,\ x_2 = 0,\ x_3 = 0$, or $x_1 = 0,\ x_2 = 1,\ x_3 = 0$, or $x_1 = 0,\ x_2 = 0,\ x_3 = 1$.

In any case,

$$\phi_1(X) \leq \alpha_1^{(0)} + \alpha_1^{(1)} + P_1^{(0)} + \sum_{j=1}^{3} P_1^{(j)} + \sum_{1\leq i\leq j\leq 3} P_1^{(ij)}$$

$$(= a,\ \text{say})$$

Similarly,

$$\phi_2(X) \leq \alpha_2^{(0)} + \alpha_2^{(1)} + P_2^{(0)} + \sum_{j=1}^{3} P_2^{(j)} + \sum_{1\leq i\leq j\leq 3} P_2^{(ij)}$$

$$(= b, \text{ say})$$

$$\phi_3(X) \leq \alpha_3^{(0)} + \alpha_3^{(1)} + P_3^{(0)} + \sum_{j=1}^{3} P_3^{(j)} + \sum_{1\leq i\leq j\leq 3} P_3^{(ij)}$$

$$(= c, \text{ say})$$

Hence, the conditions for $\Phi(D) \subset D^3$ are:

i) $\sum_{j=1}^{3} q_l^{(j)} \geq 0,\ l = 1,\ 2,\ 3$

ii) $\sum_{1\leq i,j\leq 3} q_l^{(ij)} \geq 0,\ l = 1,\ ,2,\ 3$

iii) $a \leq 1,$

iv) $b \leq 1,$

v) $c \leq 1.$

The above argument can be extended to prove that our n-species general population model given by (2.1-2.10) has fixed points. Thus we have essentially proved the following theorem:

Theorem 2.0.3. *The n-species general discrete population model given by (2.1-2.10) has a fixed point if the following conditions are satisfied:*

i) $\sum_{j=1}^{n} q_l^{(j)} \geq 0,\ l = 1,\ 2,\ 3, \cdots,\ n$

ii) $\sum_{1\leq i,j\leq n} q_l^{(ij)} \geq 0,\ l = 1,\ 2,\ 3, \cdots,\ n$

iii) $a_l \leq 1,$ *where* $a_l = \alpha_l^{(0)} + \alpha_l^{(1)} + P_l^{(0)} + \sum_{j=1}^{n} P_l^{(j)} + \sum_{1\leq i\leq j\leq n} P_l^{(ij)},\ l = 1,\ 2,\ 3, \cdots,\ n$

We note that the fixed point in the below need not be unique. For example, the following 2-species model satisfies the hypotheses of Theorem 2.0.3, and it is easy to see that it has infinitely many fixed points in the interior of the first quadrant:

$$x_{k+1} = x_k(x_k + y_k + 0.5)$$

$$y_{k+1} = y_k(x_k + y_k + 0.5)$$

CHAPTER 3

PIONEER-CLIMAX MODELS

Those species that first colonize a barren land are called *pioneer-species*. They are very hardy species that have adapted themselves to harsh conditions of nature, such as soil with less water retaining properties, and an overall dearth of water. To survive such harsh environments, in the course of time they tend to develop longer roots, leaves that transpire less, and other such adaptations. They are also the ones that usually grow first in an ecosystem which is destroyed by a forest fire, flood, earthquake, volcanic eruption or human intervention such as clearance of land for development and mining. They grow rapidly, but excessive increases in their density are detrimental to their own growth, leading ultimately to extinction. As the ecosystem grows with time, new species called *climax-species* take over from the pioneer species. They now share the environment which was first occupied by the pioneer species. But they take more time to grow. The initial low density of climax species enhances their growth. Once they attain their maximum density, their growth rate starts to decline. Some examples of pioneer species are weeds, marram grass, some types of Pine and Poplar trees, wind-dispersed microbes, mosses and lichens that grow close to the ground. Hardwood trees like Oak, Maple, and White Spruce are examples of climax species. For more details, see[38, 39, 47].

In an ecosystem, there are many interactions taking place such as animal-animal, plant-plant, plant-animal which either lead to decline and possible extinction of one or more of the species (Survival of the Fittest) or in co-existence (Symbiosis). There also is another scenario, where some particular species of plants survive the harsh conditions (pioneer) of the environment and later on become extinct before making the environment more friendly for other species (climax), thus increasing their chances

for survival. In the jargon of ecology this is called *succession.* But after attaining maximum density, the climax species also start to dwindle. For more details, see [38, 39, 47].

This dissertation is inspired by the work of such researchers as Selgrade and Namkoong [38, 39], Franke and Yakubu [12], Suzanne Sumner [47], and Commins and Hassel [18]. These authors usually combine all the individual population densities x_i of different species into a single entity, called the *total weighted density*, $z_i = \sum_{j=1}^{n} c_{ij}x_i(n)$, where the $|c_{ij}|$ represent the intensity of the effect of the $j-$th population on the $i-$th. This helps to take into account all the competition (both interspecies and intraspecies) which takes place among the species. So, while modeling an individual species, we will consider per capita growth rates to be functions of total weighted density. This is called the *fitness function.* In Figure 3.1, the *fitness function* is:

$$h(x) = e^{a-x}$$

where, a is a parameter which determines whether a species will have a pioneer or climax growth. For the ith species to be a pioneer, it is required that the fitness function h_i is smooth, monotonically decreasing and satisfies $h_i(0) > 1$. On the other hand, the species is climax if h_i is smooth, initially monotonically increasing, reaches some maximum density, and deceases monotonically thereafter. Typical growth of pioneer and climax species is shown in Figure 3.1. A widely accepted and studied 2-species pioneer-climax discrete model was introduced in Selgrade and Namkoong [38, 39]. Extending it to 3-dimensions with some generalization, we take the following as our 3-D pioneer-climax discrete model - the model upon which we shall hereafter

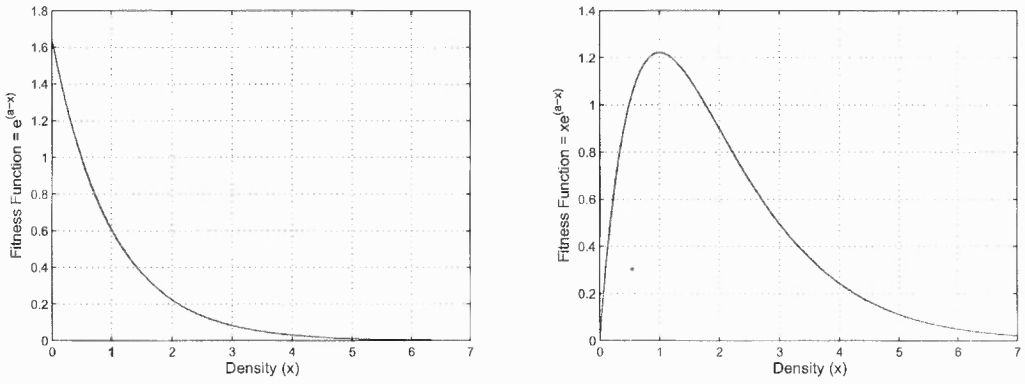

(a) Pioneer growth, with parameter $a = 0.5$ (b) Climax growth, with parameter $a = 1.2$

Figure 3.1 Growth of pioneer and climax species.

focus our analysis.

$$\begin{aligned} x_1(n+1) &= x_1(n) z_1^{m_1} e^{a-z_1} \\ x_2(n+1) &= x_2(n) z_2^{m_2} e^{b-z_2} \\ x_3(n+1) &= x_3(n) z_3^{m_3} e^{c-z_3} \end{aligned} \tag{3.1}$$

where

$$z_i = \sum_{j=1}^{n} c_{ij} x_i(n),$$

is the total weighted density, with all interaction coefficients $c_{ij} \geq 0$,

$m_i = 0, \implies x_i$ is a pioneer species

$m_i = 1,$ with respective a, b or $c > 1, \implies x_i$ is a climax species, and

Clearly this model is a particular case of the general model introduced in the previous section.

To make our results more relevant to real world ecosystems, we shall further concentrate our attention by imposing *hierarchical competition* [5] on our model.

In hierarchical competition, a species i will affect the growth of another species j if the jth species lies below the ith in the food chain of the ecosystem under consideration. To be more precise, our pioneer-climax discrete model with hierarchical competition reduces to

$$\begin{aligned} x_1(n+1) &= x_1(n)(c_{11}x_1(n))^{m_1}e^{a-c_{11}x_1(n)} \\ x_2(n+1) &= x_2(n)(c_{21}x_1(n)+c_{22}x_2(n))^{m_2}e^{b-c_{21}x_1(n)-c_{22}x_2(n)} \\ x_3(n+1) &= x_3(n)(c_{31}x_1(n)+c_{32}x_2(n)+c_{33}x_3(n))^{m_3}e^{c-c_{31}x_1(n)-c_{32}x_2(n)-c_{33}x_3(n)} \end{aligned} \tag{3.2}$$

Our 3-dimensional pioneer-climax hierarchical model exhibits a variety of behaviors that one can expect in any discrete dynamical population model such as extinction (or competitive exclusion), permanencies, stability, periodic orbits, bifurcations and finally chaos. Figure 2, which shows the iterates of the three coordinates, illustrates some of these behaviors.

Before moving on to a more detailed analysis, we make some general observations about the mappings (3.1) and (3.2). It is easy to see that the following sets are (positively) invariant for these maps: $\mathbf{R}^3_+$; and all the non-negative coordinate axes and coordinate planes. Moreover, in regions where these maps are invertible, these same sets are completely invariant. Physically speaking, the positive invariance of $\mathbf{R}^3_+$ is a necessity, since there are no populations of negative size.

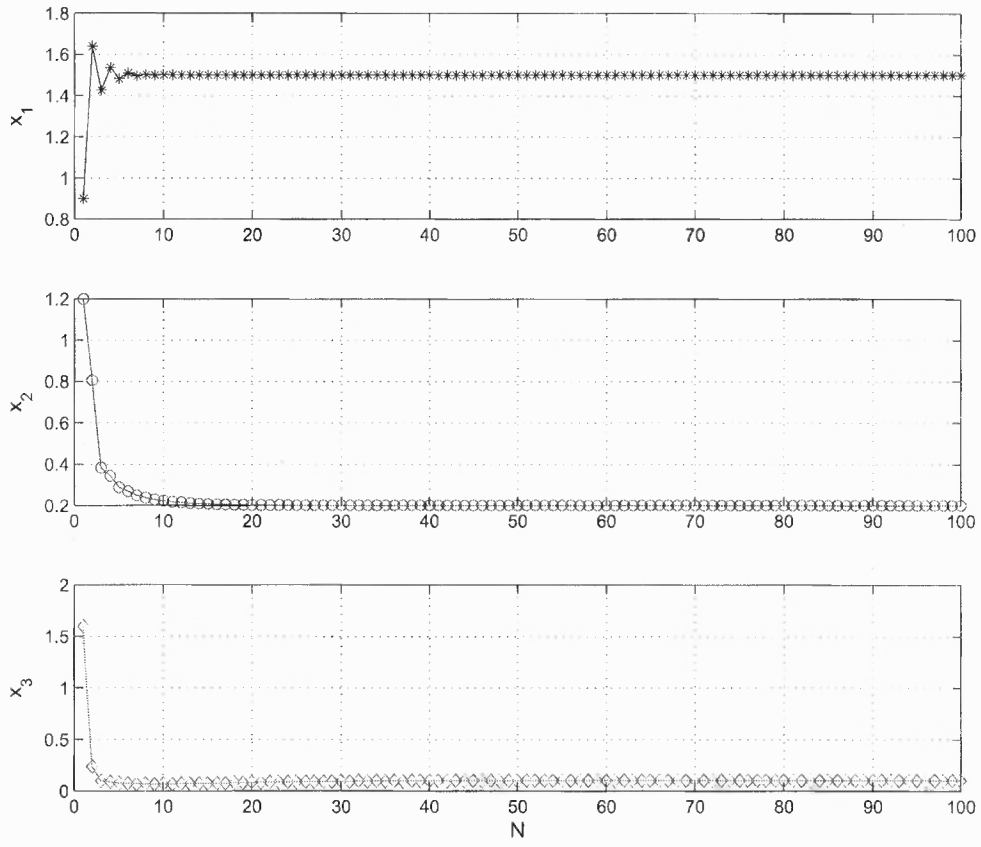

Figure 3.2 Stabilizing behavior is observed for the all-pioneer hierarchical model. The three species x_1, x_2 and x_3 have initial densities as 0.9, 1.2 and 1.6 respectively. The parameters a, b and c are 1.5, 1.7 and 1.8 respectively. The interspecies and intraspecies interaction coefficients are 1.

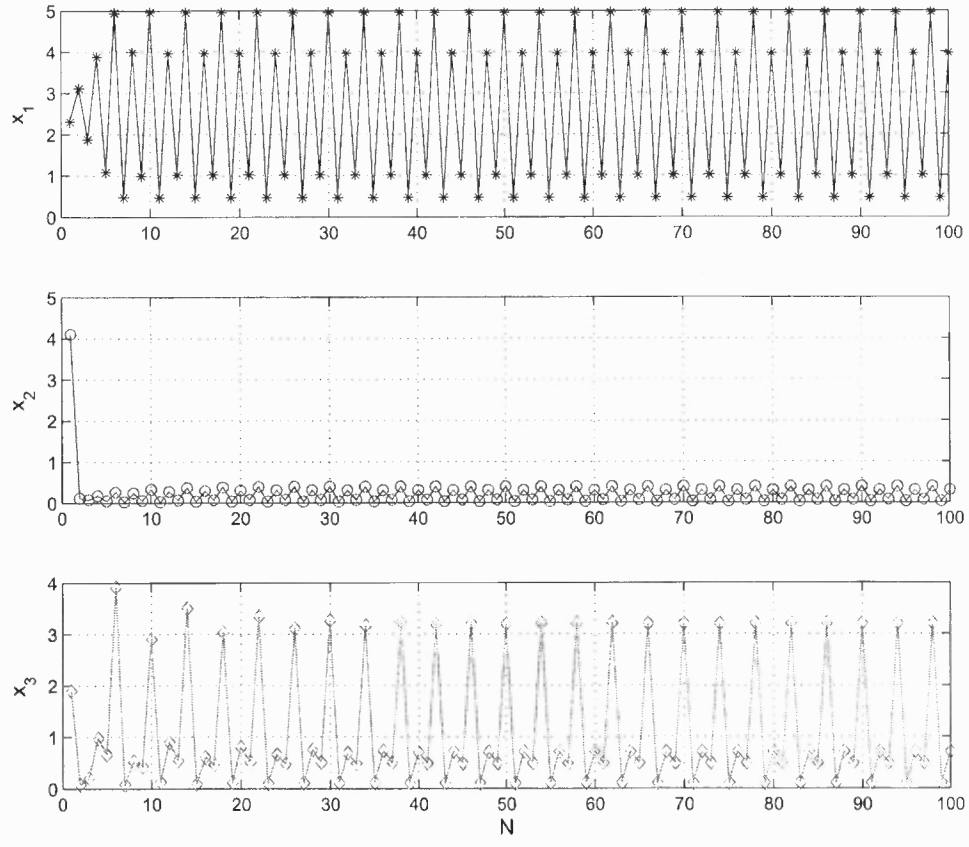

Figure 3.3 Periodic behavior is observed for the 3 - dimensional pioneer - climax hierarchical model. The three species x_1, x_2 and x_3 have 2.3, 4.1 and 1.9 respectively as initial densities. The pioneer species are represented by x_1 and x_2 while x_3 is the climax species. The parameters a, b and c are 2.6, 2.8 and 3.0 respectively. Here orbits of period 4 are observed. The interspecies and intraspecies interaction coefficients are 1.

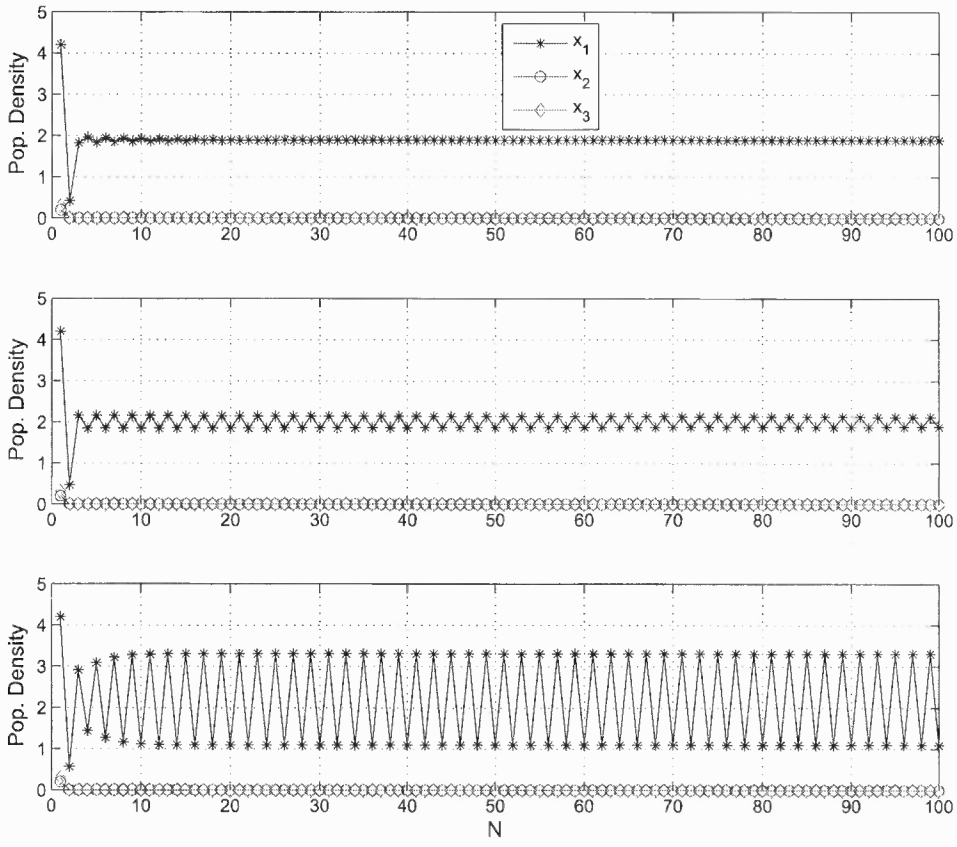

Figure 3.4 Period-doubling behavior is observed for the all - pioneer hierarchical model. The three species x_1, x_2 and x_3 have initial densities as 4.2, 0.2 and 0.3 respectively. The parameters b, c are 0.1 while bifurcation parameter a takes values 1.89, 2 and 2.2. The interspecies and intraspecies interaction coefficients are 1.

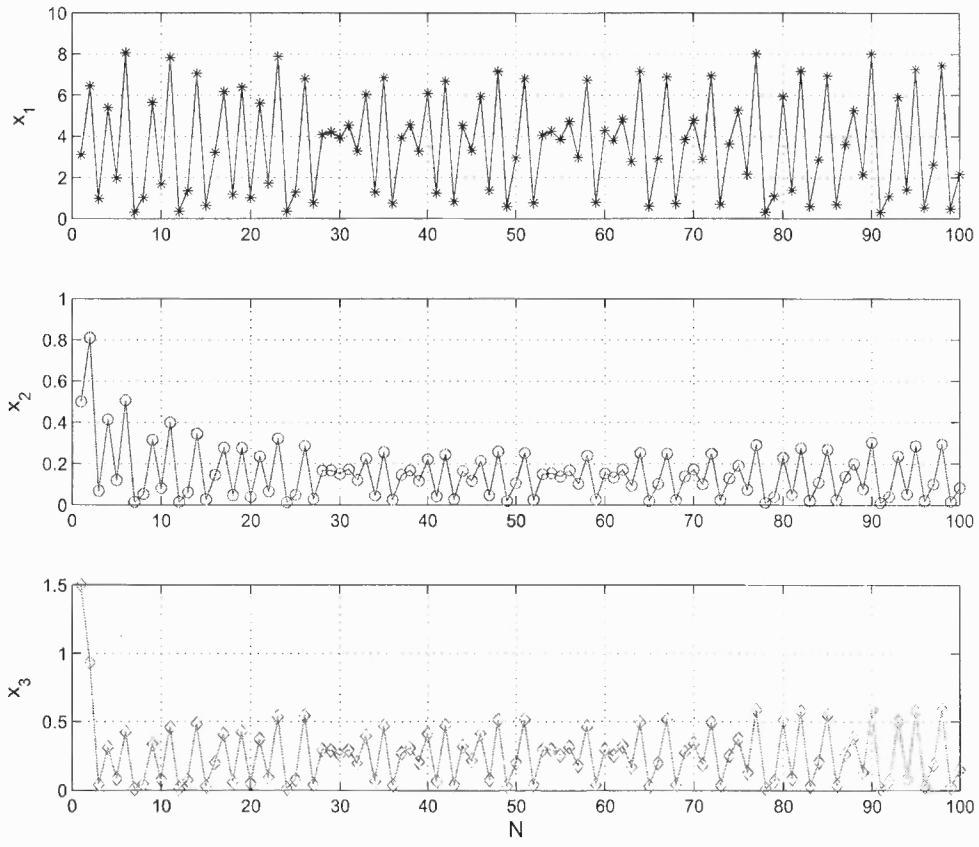

Figure 3.5 Chaotic behavior is observed for the all - climax hierarchical model. The three species x_1, x_2 and x_3 have 3.1, 0.5 and 1.5 respectively as initial densities. The parameters a, b and c are 2.7, 2.8 and 3 respectively. The interspecies and intraspecies interaction coefficients are 1.

CHAPTER 4

LOCAL STABILITY ANALYSIS OF 3-DIMENSIONAL PIONEER-CLIMAX MODEL

Usually the first thing to do in order to study any dynamical system is to find its fixed points. So, we now proceed to find the fixed points for our 3-dimensional hierarchical pioneer-climax model. As we have 3-dimensions representing species types that are either pioneer or climax, we have 2^3 combinations. First, we shall do the calculations for the all-pioneer case. The n-dimensional all- pioneer hierarchical model can be written as:

$$\begin{aligned}
x_1(k+1) &= x_1(k)e^{a_1 - c_{11}x_1(k)} \\
x_2(k+1) &= x_2(k)e^{a_2 - c_{21}x_1(k) - c_{22}x_2(k)} \\
\vdots \quad &= \qquad\qquad \vdots \\
x_n(k+1) &= x_n(k)e^{a_n - c_{n1}x_1(k) - c_{n2}x_2(k) - \cdots - c_{nn}x_n(k)}
\end{aligned}$$

The 3-dimensional all pioneer hierarchical model has the form:

$$\begin{aligned}
x_1(n+1) &= x_1(n)e^{a - c_{11}x_1(n)} \\
x_2(n+1) &= x_2(n)e^{b - c_{21}x_1(n) - c_{22}x_2(n)} \\
x_3(n+1) &= x_3(n)e^{c - c_{31}x_1(n) - c_{32}x_2(n) - c_{33}x_3(n)}
\end{aligned} \tag{4.1}$$

Any fixed point $(x_1^*,\ x_2^*,\ x_3^*)$ must satisfy

$$x_i^*(n+1) = x_i^*(n), \quad i = 1,\ 2,\ 3$$

so we have:

$$x_1^* e^{a-c_{11}x_1^*} = x_1^* \tag{4.2}$$

$$x_2^* e^{b-c_{21}x_1^*-c_{22}x_2^*} = x_2^* \tag{4.3}$$

$$x_3^* e^{c-c_{31}x_1^*-c_{32}x_2^*-c_{33}x_3^*} = x_3^* \tag{4.4}$$

(4.2) $\Longrightarrow$ $x_1^* = 0$, $x_1^* = \frac{a}{c_{11}}$. Substituting $x_1^* = 0$ in (4.3), we get $x_2^* = 0$, $x_2^* = \frac{b}{c_{22}}$. Now substituting $x_1^* = 0$, $x_2^* = 0$ in (4.4), we get $x_3^* = 0$, $x_3^* = \frac{c}{c_{33}}$.

Thus, $(0,0,0)$ and $(0,0,\frac{c}{c_{33}})$ are two of the fixed points. Now substituting $x_1^* = 0$, $x_2^* = \frac{b}{c_{22}}$ in (4.4), we get $x_3^* = 0$, $x_3^* = c - \frac{bc_{33}}{c_{22}} (= \beta)$.

So, we have $(0,\frac{b}{c_{22}},0)$ and $(0,\frac{b}{c_{22}},\ \beta)$ as two more fixed points. Substituting $x_1^* = \frac{a}{c_{11}}$ in (4.3),, we get $x_2^* = 0$, $x_2^* = \frac{b}{c_{22}} - \frac{c_{21}a}{c_{11}c_{22}} (= \frac{\alpha}{c_{22}})$.

Substituting $x_1 = \frac{a}{c_{11}}$, $x_2^* = 0$ in (4.4),, we get $x_3^* = 0$, $x_3^* = \frac{c}{c_{33}} - \frac{c_{31}a}{c_{11}c_{33}} (= \frac{\gamma}{c_{33}})$

So, $(\frac{a}{c_{11}},\ 0,\ 0)$ and $(\frac{a}{c_{11}},\ 0,\ \frac{\gamma}{c_{33}})$ as two more fixed points. Finally, substituting $x_1^* = \frac{a}{c_{11}}$, $x_2^* = \frac{\alpha}{c_{22}}$ in (4.4) we get $(\frac{a}{c_{11}},\ \frac{\alpha}{c_{22}},\ 0)$ and $(\frac{a}{c_{11}},\ \frac{\alpha}{c_{22}},\ \frac{\delta}{c_{33}})$, where $\delta = c - \frac{ac_{31}}{c_{11}} - \frac{\alpha c_{32}}{c_{22}}$ as two more fixed points.

Hence, in total we have eight possible fixed points for the 3-dimensional all pioneer hierarchical model. They are:

$(0,0,0)$, $(0,0,\frac{c}{c_{33}})$, $(0,\frac{b}{c_{22}},0)$, $(0,\frac{b}{c_{22}},\beta)$, $(\frac{a}{c_{11}},\ 0,\ 0)$, $(\frac{a}{c_{11}},\ 0,\ \frac{\gamma}{c_{33}})$, $(\frac{a}{c_{11}},\ \frac{\alpha}{c_{22}},\ 0)$ and $(\frac{a}{c_{11}},\ \frac{\alpha}{c_{22}},\ \frac{\delta}{c_{33}})$ where $\delta = c - \frac{ac_{31}}{c_{11}} - \frac{\alpha c_{32}}{c_{22}}$

It should be clear that the all-pioneer case is the only case which can be generally fully solved in simple form analytically to get all its possible fixed points. To show this, we now consider a 3-dimensional hierarchical model with two pioneer and one climax species, given in the form:

$$\begin{aligned} x_1(n+1) &= x_1(n)e^{a-c_{11}x_1(n)} \\ x_2(n+1) &= x_2(n)e^{b-c_{21}x_1(n)-c_{22}x_2(n)} \\ x_3(n+1) &= x_3(n)(c_{31}x_1(n) + c_{32}x_2(n) + c_{33}x_3(n))e^{c-c_{31}x_1(n)-c_{32}x_2(n)-c_{33}x_3(n)} \end{aligned} \tag{4.5}$$

We observe that it is convenient to view this system in terms of iterates of a map - depending on the types, denoted in terms of the powers of the z_i as $\mathbf{m} := (m_1, m_2, m_3)$, and all the system parameters, which we lump together as a parameter vector defined as $\boldsymbol{\mu} := (a, b, c, c_{11}, \ldots, c_{33})$ - defined as

$$T = T_{\mathbf{m},\boldsymbol{\mu}} : \mathbf{R}_+^3 \to \mathbf{R}_+^3,$$

where

$$T_{\mathbf{m},\,\boldsymbol{\mu}}(x_1(n),\ x_2(n),\ x_3(n)) := (x_1(n+1),\ x_2(n+1),\ x_3(n+1))$$

Observe that the particular case of this map for the above system has $\mathbf{m} := (0, 0, 1)$, indicating two pioneer species, followed by a climax species, and $\boldsymbol{\mu} := (a, b, c, c_{11}, 0, 0, c_{21}, c_{22}, 0, c_{31}, c_{32}, c_{33})$. Proceeding as in the previous case, the fixed points (x_1^*, x_2^*, x_3^*) satisfy

$$x_i^*(n+1) = x_i^*(n) \text{ for } i = 1, 2, 3.$$

So, we get

$$x_1^* e^{a - c_{11}x_1^*} = x_1^* \tag{4.6}$$

$$x_2^* e^{b - c_{21}x_1^* - c_{22}x_2^*} = x_2^* \tag{4.7}$$

$$x_3^*(c_{31}x_1^*(n) + c_{32}x_2^*(n) + c_{33}x_3^*(n))e^{c - c_{31}x_1^* - c_{32}x_2^* - c_{33}x_3^*} = x_3^* \tag{4.8}$$

It follows from (4.6) that $x_1^* = 0$, and if $x_1^* \neq 0$, then $e^{a - c_{11}x_1^*} = 1$, which implies that $a - c_{11}x_1^* = 0$ - and this is only possible if $c_{11} > 0$, which implies $x_1^* = a/c_{11}$. Now substituting $x_1^* = 0$ in (4.7), we get $x_2^* = 0$ or $x_2^* = \frac{b}{c_{22}}$, assuming $c_{22} > 0$. Upon substituting $x_1^* = 0$, $x_2^* = 0$ in (4.8), we obtain $x_3^* = 0$. Hence $(0, 0, 0)$ is one of

the fixed points. The x_3 coordinate of the other fixed point satisfies the equation:

$$\begin{aligned} c_{33}x_3^* e^{c-c_{33}x_3^*} &= 1 \\ -c_{33}x_3^* e^{c-c_{33}x_3^*} &= -1 \\ -c_{33}x_3^* e^{-c_{33}x_3^*} &= -\frac{1}{e^c} \\ -c_{33}x_3^* &= W(-\frac{1}{e^c}), \end{aligned} \tag{4.9}$$

where the *Lambert W* function [6] is the inverse function, defined for $x > -1$ and $f(x) > -e^{-1}$ of $f(x) = xe^x$ and $x = ye^y \iff y = W(x)$

Hence,

$$x_3^* = \frac{-W(-\frac{1}{e^c})}{c_{33}}, \tag{4.10}$$

which requires that $c \geq 1$ so that W is defined.

Similarly if we substitute $x_1^* = 0$, $x_2^* = \frac{b}{c_{22}}$ in (4.8), we find that $x_3^* = 0$. Accordingly $(0, \frac{b}{c_{22}}, 0)$ is another fixed point. The x_3 coordinate of the other fixed point satisfies the equation:

$$\begin{aligned} (\frac{c_{32}b}{c_{22}} + c_{33}x_3^*)e^{c-\frac{c_{32}b}{c_{22}}-c_{33}x_3^*} &= 1 \\ -(\frac{c_{32}b}{c_{22}} + c_{33}x_3^*)e^{c-\frac{c_{32}b}{c_{22}}-c_{33}x_3^*} &= -1 \\ -(\frac{c_{32}b}{c_{22}} + c_{33}x_3^*)e^{-\frac{c_{32}b}{c_{22}}-c_{33}x_3^*} &= -\frac{1}{e^c} \\ -\frac{c_{32}b}{c_{22}} - c_{33}x_3^* &= W(-\frac{1}{e^c}) \end{aligned} \tag{4.11}$$

Hence,

$$x_3^* = -\frac{c_{32}b + c_{22}W(-e^{-c})}{c_{33}c_{22}} \tag{4.12}$$

In similar fashion we can find all the remaining fixed points for this two pioneer and one climax hierarchical model and all other combinations of pioneer and climax

hierarchical models. For reference, we list all of the fixed points of the above system: $(0,\ 0,\ 0)$, $(0,\ 0,\ \frac{b}{c_{22}})$, $(\frac{a}{c_{11}},\ 0,\ 0)$, $(\frac{a}{c_{11}},\ \frac{\alpha}{c_{22}},\ 0)$, $(0, 0, -W(\frac{e^{-c}}{c_{33}}))$, $(0, \frac{b}{c_{22}}, -\frac{bc_{32}+c_{22}W(e^{-c})}{c_{22}c_{33}})$, $(\frac{a}{c_{11}}, 0, -\frac{ac_{31}+c_{11}W(e^{-c})}{c_{11}c_{33}})$, $(\frac{a}{c_{11}},\ \frac{\alpha}{c_{22}}, -\frac{ac_{31}c_{22}+\alpha c_{32}c_{11}c33+c_{11}c_{22}W(e^{-c})}{c_{11}c_{22}c_{33}})$ where $\alpha = b - \frac{ac_{21}}{c_{11}}$.

We note here also that the invariance mentioned in the previous section can be indicated very neatly using the mapping representation; namely as $T_{\mathbf{m},\mu}\left(\mathbf{R}^3_+\right) \subset \mathbf{R}^3_+$, $T_{\mathbf{m},\mu}\,(\text{coordinate line}) \subset \text{coordinate line}$, and $T_{\mathbf{m},\mu}\,(\text{coordinate plane}) \subset \text{coordinate plane}$.

4.1 Local Stability Analysis

Once we have the fixed points for a dynamical system, we then shift our focus to the local stability of the system about those fixed points. We illustrate this by doing the local stability analysis for the fixed point $(\frac{a}{c_{11}},\ \frac{\alpha}{c_{22}},\ \frac{\delta}{c_{33}})$, where $\delta = c - \frac{ac_{31}}{c_{11}} - \frac{\alpha c_{32}}{c_{22}}$ The mapping defined by (4.1) is:

$$x_1(n+1) = x_1(n)e^{a-c_{11}x_1(n)}$$

$$x_2(n+1) = x_2(n)e^{b-c_{21}x_1(n)-c_{22}x_2(n)}$$

$$x_3(n+1) = x_3(n)e^{c-c_{31}x_1(n)-c_{32}x_2(n)-c_{33}x_3(n)}$$

The Jacobian J of the above system, which is just the matrix representation of the derivative $T'_{\mathbf{m},\mu}$, is:

$$J = \begin{bmatrix} (1-c_{11}x_1)e^{a-c_{11}x_1} & 0 & 0 \\ (-x_2c_{21}e^{b-c_{21}x_1-c_{22}x_2} & (1-c_{22}x_2)e^{b-c_{21}x_1-c_{22}x_2} & 0 \\ (-x_3c_{31}e^{c-c_{31}x_1-c_{32}x_2-c_{33}x_3} & (-x_3c_{32}e^{c-c_{31}x_1-c_{32}x_2-c_{33}x_3} & (1-c_{33}x_3)e^{c-c_{31}x_1-c_{32}x_2-c_{33}x_3} \end{bmatrix}$$

The Jacobian J evaluated at the fixed point $(\frac{a}{c_{11}},\ \frac{\alpha}{c_{22}},\ \frac{\delta}{c_{33}})$ is:

$$J = \begin{bmatrix} (1-a) & 0 & 0 \\ (-\frac{\alpha}{c_{22}}c_{21})e^{b-c_{21}\frac{a}{c_{11}}-\alpha} & (1-\alpha)e^{b-c_{21}\frac{a}{c_{11}}-\alpha} & 0 \\ (\frac{-\delta}{c_{33}}c_{31})e^{c-c_{31}\frac{a}{c_{11}}-c_{32}\frac{\alpha}{c_{22}}-\delta} & (-\frac{\delta}{c_{33}}c_{32})e^{c-c_{31}\frac{a}{c_{11}}-c_{32}\frac{\alpha}{c_{22}}-\delta} & (1-\delta)e^{c-c_{31}\frac{a}{c_1}-c_{32}\frac{\alpha}{c_{22}}-\delta} \end{bmatrix}$$

As this is a lower triangular matrix (due to the hierarchical structure), the diagonal elements are the eigenvalues λ of the above matrix. Hence for linear stability we need

$$|\lambda_i| < 1, \qquad \text{for } i = 1, 2, 3$$

which requires that

$$|1-a|,\ |(1-\alpha)|e^{b-c_{21}\frac{a}{c_{11}}-\alpha},\ |(1-\delta)|e^{c-c_{31}\frac{a}{c_1}-c_{32}\frac{\alpha}{c_{22}}-\delta} < 1$$

Similarly, we can check the stability condition for other fixed points too.

There can be numerous other situations, such as two of the eigenvalues say $\lambda_1,\ \lambda_2$ are greater than 1 in magnitude, and λ_3 is less than 1 in magnitude. In this case we have a 1-dimensional stable manifold initially in the x_3-direction and a 2-dimensional unstable manifold tangent to the $x_1,\ x_2$-plane at the fixed point. This means the x_3 species is linearly stable while $x_1,\ x_2$ species will be linearly unstable.

Lemma 4.1.1. *For the 3-dimensional all-pioneer model,* $(0,\ 0,\ 0)$ *is a repeller if* $a > 0,\ b > 0$ *and* $c > 0$, *and an attractor if* $a < 0,\ b < 0$ *and* $c < 0$. *Note that we have assumed* $a, b, c > 0$.

Proof. The Jacobian of (4.1) evaluated at $(0,\ 0,\ 0)$ is

$$J = \begin{bmatrix} e^a & 0 & 0 \\ 0 & e^b & 0 \\ 0 & 0 & e^c \end{bmatrix}$$

The origin will be a repeller if

$$e^a,\ e^b,\ e^c > 1,$$

which implies that

$$a,\ b,\ c > 0,$$

and an attractor if

$$e^a,\ e^b,\ e^c < 1$$

which implies that

$$a,\ b,\ c < 0.$$

This yields the desired result. □

4.2 Invariance and Stability

Given the relatively simple form of (4.1), it makes sense to look for invariant sets besides the fixed points that offer insights into stability properties of the dynamics. For example, it follows directly from the definition of the map that the plane

$$P = \{x = (x_1,\ x_2,\ x_3)\ \in\ \mathbf{R}^3 :\ x_1 = a/c_{11}\} \tag{4.13}$$

is invariant. Therefore, (4.1) reduces to a 2-dimensional system when restricted to P. Moreover, the plane P attracts or repels all nearby orbits if $|1-a| < 1$ or $|1-a| > 1$, respectively. Naturally this invariance and the stability of the invariant plane yields a significant amount of information about the overall dynamics of the system.

More generally, analogous properties apply to any fixed point of the first-coordinate map in any all-pioneer hierarchical model. In particular, any fixed point x_1^* of the first-coordinate map

$$x_1 \rightarrow f_1(x_1) = x_1 e^{a - c_{11} x_1} \tag{4.14}$$

has a corresponding invariant plane

$$P(x_1^*) = \{x = (x_1,\ x_2,\ x_3)\ \in\ \mathbf{R}^3 : x_1 = x^*\}, \tag{4.15}$$

and this plane is a local attractor or repeller if $|f_1'(x_1^*)| < 1$ or $|f_1'(x_1^*)| > 1$, respectively. We note that $x_1 = 0$ is always a fixed point of (4.14), and there is a positive fixed point at $x_1 = a/c_{11}$.

There also are a similar set of invariance and stability properties if the first-coordinate function of the hierarchical 3-dimensional system is of climax form

$$x_1 \rightarrow g_1(x_1) = x_1^2 e^{a - c_{11}x_1} \tag{4.16}$$

The map g_1 always has $x_1 = 0$ as a fixed point. It is easy to see that $x_2 = 0$ is the only nonnegative fixed point of g_1 if $a < 1 + \log(c_{11})$ and there is another fixed point at $x_1 = 1/c_{11}$ when $a = 1 + \log(c_{11})$, and a pair of positive fixed points on either side of $1/c_{11}$ when $a > 1 + \log(c_{11})$. In all of these cases there are corresponding invariant planes of the form (4.15) owing to the hierarchical nature of the system. Observe that the invariant (coordinate) plane $P(0)$ is always a superstable attractor since $g_1' = 0$.

CHAPTER 5

PERIODIC BEHAVIOR

The environment is continuously changing. However, there are some ecosystems, both of fauna and flora, in which various states tend to repeat themselves periodically. For example, a succession of climax species over pioneer species that is observed year after year indicates a basic cyclic trend in various ecosystems. Thus periodic behavior in such systems is a very revealing indicator of the ways in which they evolve, and especially important are stable periodic solutions as they identify persistent cyclic states. Furthermore, there are natural links between stable cycles in discrete dynamical models and periodic and traveling wave solutions of the more accurate partial and ordinary differential equation models that they are often devised to approximate.

In 3-dimensional hierarchical pioneer-climax models, there is usually a preponderance of periodic orbits of period 2^m generated by period doubling bifurcations, so we shall treat these cases first, restricting our attention to all-pioneer systems of the form

$$\begin{aligned} x_1(n+1) &= x_1(n)e^{a-c_{11}x_1(n)} \\ x_2(n+1) &= x_2(n)e^{b-c_{21}x_1(n)-c_{22}x_2(n)} \\ x_3(n+1) &= x_3(n)e^{c-c_{31}x_1(n)-c_{32}x_2(n)-c_{33}x_3(n)} \end{aligned} \tag{5.1}$$

where $a,\ b,\ c$ and all c_{ij} are nonnegative constants. It is convenient to use the following mapping notation to analyze periodic orbits:

$$\begin{aligned} T_{0,\,\mu} &= T_{0,\,\mu}(x_1,\ x_2,\ x_3) \\ &= (f_1(x_1;\ a,\ c_{11}),\ f_2(x_1,\ x_2;\ b,\ c_{21},\ c_{22}),\ f_3(x_1,\ x_2,\ x_3;\ c,\ c_{31},\ c_{32},\ c_{33})) \end{aligned}$$

$$= (x_1 e^{a - c_{11}x_1},\ x_2 e^{b - c_{21}x_1 - c_{22}x_2},\ x_3 e^{c - c_{31}x_1 - c_{32}x_2 - c_{33}x_3})$$

A periodic orbit of period-1, or 1-cycle, is just the set $\{x_*\}$ containing the fixed point x_* satisfying

$$T_{0,\,\mu}(x_*) = x_*$$

More generally, if m is an integer greater than 1, a periodic orbit of (least) period-m, or m-cycle is the set $x_*,\ T_{0,\,\mu}(x_*),\ \cdots,\ T_{0,\,\mu}^{m-1}(x_*)$ characterized by

$$T_{0,\,\mu}^{n}(x_*) \neq x_* \quad \text{for } 1 \leq n < m$$
$$T_{0,\,\mu}^{m}(x_*) = x_*$$

An m-cycle is linearly stable if the eigenvalues $\lambda^{(m)}$ of the derivative (or Jacobian matrix)

$$(T_{0,\,\mu}^{m})'(x_*)$$

are all interior to the unit circle in the complex plane $\mathbb{C}$, *i.e.* they satisfy $|\lambda^{(m)}| < 1$.

Our main interest is in finding stable periodic orbits of our 3-dimensional pioneer-climax systems. It follows from the hierarchical nature of the system that the Jacobian matrices above are all lower triangular, so the eigenvalues - which must be real - are just the diagonal elements. It turns out that most of the higher period cycles in the system under consideration are generated by period doubling bifurcation, so 2^k-cycles tend to be the predominant periodic orbits.

Let us first seek period-2 orbits (or 2-cycles), by considering the following transformation:

$$F^2 = \left(f_1^2(x_1,\ a),\ f_2^2(x_1,\ x_2,\ a,\ b),\ f_3^2(x_1,\ x_2,\ x_3,\ a,\ b,\ c)\right),$$

where,

$$f_1^2(x_1,\ a) = f_1(f_1(x_1,\ a),\ a)$$
$$f_2^2(x_1,\ x_2,\ a,\ b) = f_2(f_1(x_1,\ a),\ f_2(x_1,\ x_2,\ b),\ b)$$
$$f_3^2(x_1,\ x_2,\ x_3,\ a,\ b,\ c) = f_3(f_1(x_1,\ a),\ f_2(x_1,\ x_2,\ b),\ f_3(x_1,\ x_2,\ x_3\ c),\ c)$$

The period-2 orbit is stable if the eigenvalues of the Jacobian matrix of the above transformation all have magnitude less than 1. Due to the hierarchical nature of the model, the eigenvalues are the diagonal elements of the Jacobian. Using symbolic mathematics in MATLAB the eigenvalues are:

$$\lambda_1^{(2)} = X_1Y_1 - x_1c_{11}X_1Y_1 + x_1X_1(-c_{11}X_1 + c_{11}^2x_1X_1)Y_1$$
$$\lambda_2^{(2)} = X_2Y_2 - x_2c_{22}X_2Y_2 + x_2Y_2(-c_{22}X_2 + c_{22}^2x_2X_2)Y_2$$
$$\lambda_3^{(2)} = X_3Y_3 - x_3c_{33}X_3Y_3 + x_3X_3(-c_{33}X_3 + c_{22}^2x_3X_3)Y_3$$

where,

$$X_1 = e^{a-c_{11}x_1}$$
$$Y_1 = e^{a-c_{11}x_1X_1}$$
$$X_2 = e^{b-c_{21}x_1-c_{22}x_2}$$
$$Y_2 = e^{b-c_{21}x_1e^{a-c_{11}x_1}-c_{22}x_2X_2}$$
$$X_3 = e^{c-c_{31}x_1-c_{32}x_2-c_{33}x_3}$$
$$Y_3 = e^{c-c_{31}x_1e^{a-c_{11}x_1}} - c_{32}x_2e^{b-c_{21}x_1-c_{22}x_2-c_{33}x_3X_3}$$

Hence, sufficient conditions for existence of a stable period-2 orbit for the all-pioneer 3-dimensional discrete hierarchical model are that there exists a solution of $(x_1,\ x_2,\ x_3) = F^2(x_1,\ x_2,\ x_3)$, which is not a fixed point of F and satisfies

$$|\lambda_1^{(2)}| < 1,\ |\lambda_2^{(2)}| < 1,\ |\lambda_3^{(2)}| < 1$$

It follows that in this case, a stable (non-degenerate) 2-cycle is characterized by the following:

$$T^2_{0,\mu}(x_*) = x_*$$

$$T_{0,\mu}(x_*) \neq x_*$$

and the parameters μ are such that the $\lambda_i^{(2)}$, $i = 1, 2, 3$, defined above all have absolute values less than one.

We have identified several n-cycles for $n > 1$ in our hierarchical model. Illustrations of period-2 and period-4 behavior are shown in Figures 5.1 and 5.2 in terms of iterates of the coordinates of the map. In Figure 5.1, we see a period-2 orbit for a 3-dimensional pioneer-climax hierarchical model, where x_1 is pioneer and x_2 and x_3 are climax species. We observe that the behavior of period-doubling is seen after some generations have passed. The initial densities for x_1, x_2 and x_3 are 1.5, 0.5 and 1.5 respectively while the positive parameters a, b and c are 2.0, 1.9 and 2.3 respectively.

In Figure 5.2, we see a period-4 orbit for a 3-dimensional pioneer-climax hierarchical model, where x_1 is pioneer and x_2 and x_3 are climax species. In this case too the behavior of period-4 orbits is seen after some generations have passed. The initial densities for x_1, x_2 and x_3 are 2.3, 4.1 and 1.9 respectively while the positive parameters a, b and c are 2.6, 2.8 and 3.0 respectively. The interaction coefficients in Figures 5.1 and 5.2 are equal to 1.

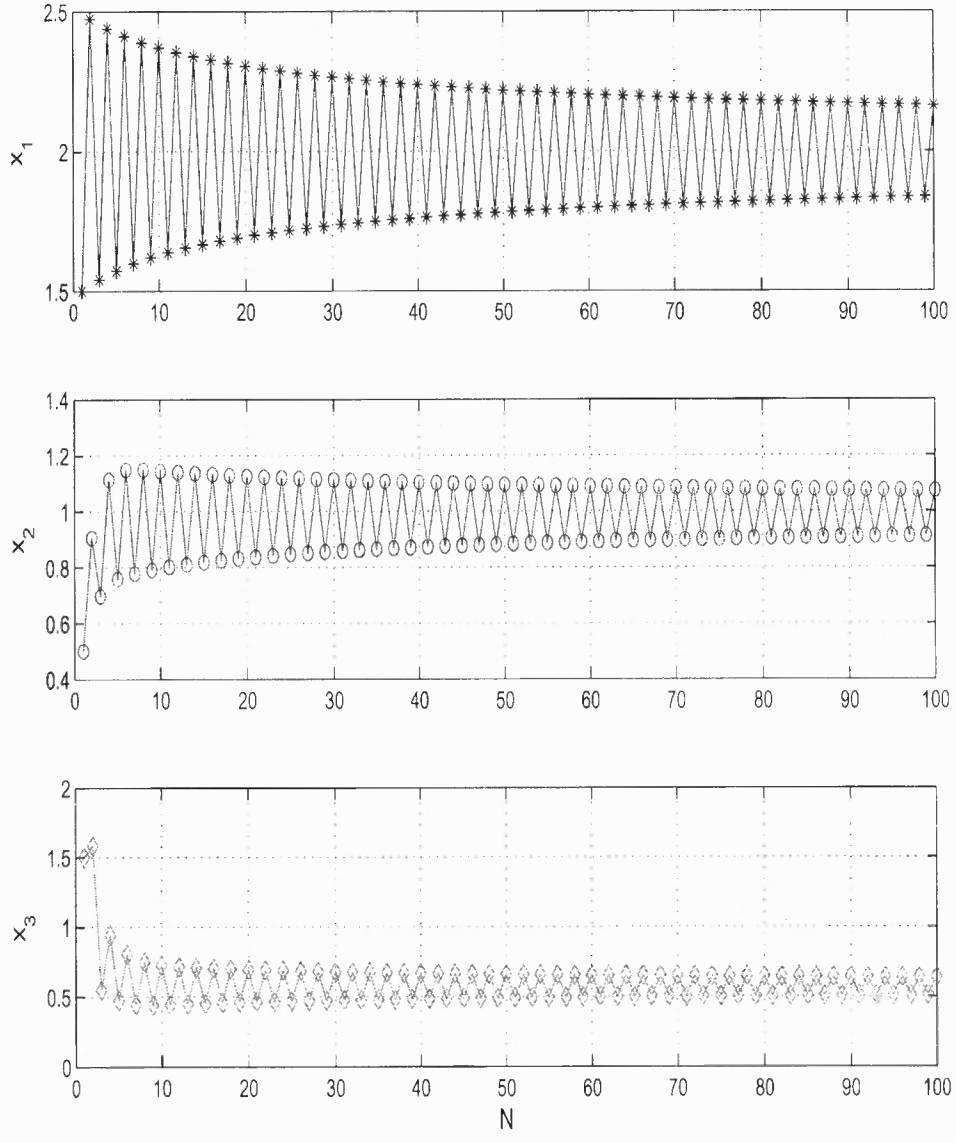

Figure 5.1 Period-2 orbits are observed for 3-dimensional pioneer-climax hierarchical model, where x_1 is pioneer and x_2 and x_3 are climax species. The initial densities for x_1, x_2 and x_3 are 1.5, 0.5 and 1.5, respectively, while the positive parameters a, b and c are 2.0, 1.9 and 2.3, respectively. The interaction coefficients are equal to 1.

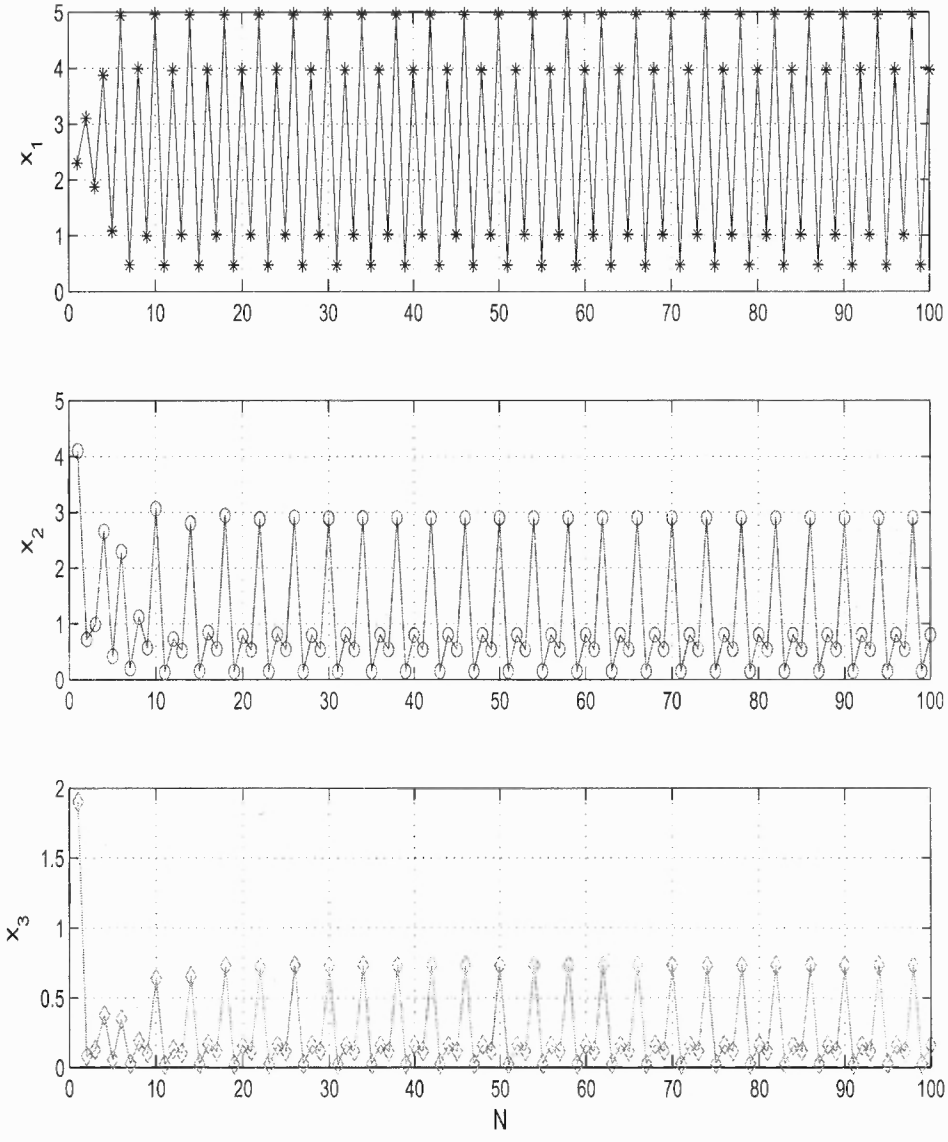

Figure 5.2 Period-4 orbits are observed for 3-dimensional pioneer-climax hierarchical model, where x_1 is pioneer and x_2 and x_3 are climax species. The initial densities for x_1, x_2 and x_3 are 2.3, 4.1 and 1.9, respectively, while the positive parameters a, b and c are 2.6, 2.8 and 3.0, respectively. The interaction coefficients are equal to 1.

We next investigate the existence of stable 3-cycles for (5.1). One advantage of the hierarchical nature of our model is that it enables us to find 3-cycles by essentially just investigating three one-dimensional maps. First, we seek a stable 3-cycle for the first component of the map $T^3_{0,\,\mu}$, which is just

$$\phi_1(x_1) := f_1^3(x_1) = f_1(f_1(f_1(x_1))),$$

where for convenience we have suppressed the parameter dependence. We can find non-fixed solutions of $x_1 = f_1^3(x_1)$ from cobweb map consideration. The cobweb map of the stable 3-cycle for x_1 is shown in Figure (5). Here $x_1(0)$ is chosen so that $x_1(1)$ is near the maximizer of f_1 where $f_1' = 0$, so that $|f_1'(x_1(2))f_1'(x_1(1))f_1'(x_1(0)| \ll 1$. To find such a point, use the cobweb map to locate an approximate $x_1(0)$ in an interval I_0 such that f_1^3 maps I_0 into itself and $|f^{3'}| < 1$ on this interval. Note that the existence of a 3-cycle for x_1 implies the existence of cycles of all periods by Sharkovsky's theorem[43], which signals chaotic dynamics owing to the work of Li and Yorke[29].

Once we have the stable 3-cycle for x_1, we seek a stable solution of

$$\phi_2(x_2) = f_2(x_1(2),\ f_2(x_1(1),\ f_2(x_1(0),\ x_2))),$$

which corresponds to a stable 3-cycle in the x_2 -coordinate corresponding to the stable 3-cycle in the x_1 -coordinate. Approximate solutions can be obtained by plotting ϕ_2 and investigating its fixed points, which can be done by using a cobweb and checking the derivative ϕ_2' to test for stability. This yields a (stable) 3-cycle for x_2 defined as

$$\phi_2(\tilde{x}_2) = \tilde{x}_2,$$

where we set

$$x_2(0) = \tilde{x}_2, \qquad x_2(1) = f_2(x_1(0),\ x_2(0)),$$
$$x_2(2) = f_2(x_1(1),\ x_2(1))$$

This can be proved in a manner analogous to that used for the stable 3-cycle for x_1; namely, using the Banach fixed theorem [2] for an approximate x_2 interval that can be identified using the cobweb map for ϕ_2.

Now that we have stable 3-cycles $\{x_1(0),\ x_1(1),\ x_1(2)\}$ and $\{x_2(0),\ x_2(1),\ x_2(2)\}$ for the coordinates x_1 and x_2, respectively, we can repeat the above procedure to find an associated stable 3-cycle for x_3. To this end, we consider the one-dimensional map

$$\phi_3(x_3) := f_3(x_1(2),\ f_2(x_1(1),\ x_2(1),\ f_3(x_1(0),\ x_2(0)),\ x_3))$$

If one finds a stable fixed point $\tilde{x_3}$ of ϕ_3, then the corresponding stable 3-cycle for x_3 is $x_3(0),\ x_3(1),\ x_3(2)$, where

$$x_3(0) = \tilde{x_3}, \qquad x_3(1) = f_3(x_1(0),\ x_2(0),\ x_3(0)),$$
$$x_3(2) = f_3(x_1(1),\ x_2(1),\ x_3(1)).$$

Then $(x_1(0),\ x_2(0),\ x_3(0))$, $(x_1(1),\ x_2(1),\ x_3(1))$, $x_1(2)$, $x_2(2)$, $x_3(2)$ is a stable 3-cycle for the discrete dynamical system (5.1).

We note that the existence of a stable 3-cycle of (5.1) for some parameter range can alternatively be proved in a three-dimensional manner by finding a rectangular region R in $\mathbb{R}^3$ such that $T^3_{0,\,\mu}(\mathrm{R}) \subset \mathrm{R}$ and T^3 is a contraction map on R. A representative result concerning 3-cycles is the following, which is illustrated in time series plots for the coordinates in Figures 5.3 and 5.4.

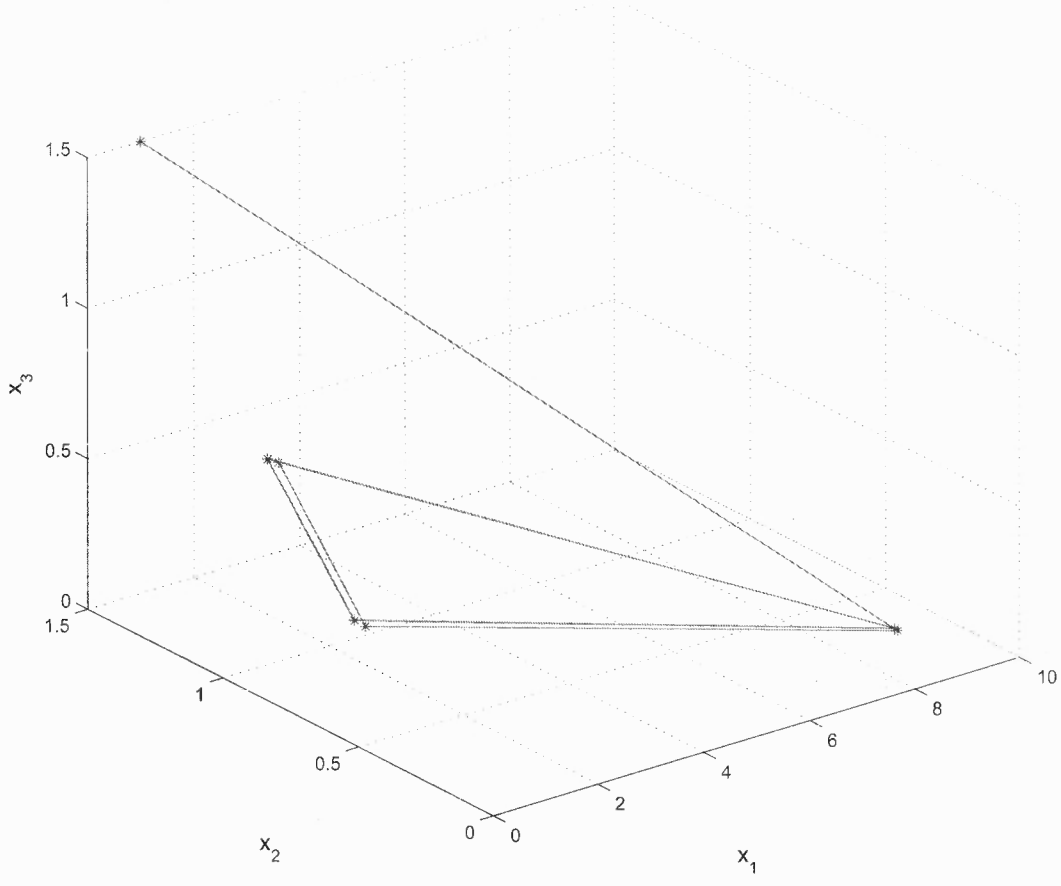

Figure 5.3 Period-3 orbit for 3-dimensional all-pioneer hierarchical model with $a = 3.1167$, $b = 1.5$, $c = 1.5$. The initial densities for x_1, x_2 and x_3 are 1, 1.5 and 1.5, respectively. The intraspecies interactions are equal to 1 and interspecies interactions are equal to 0.3.

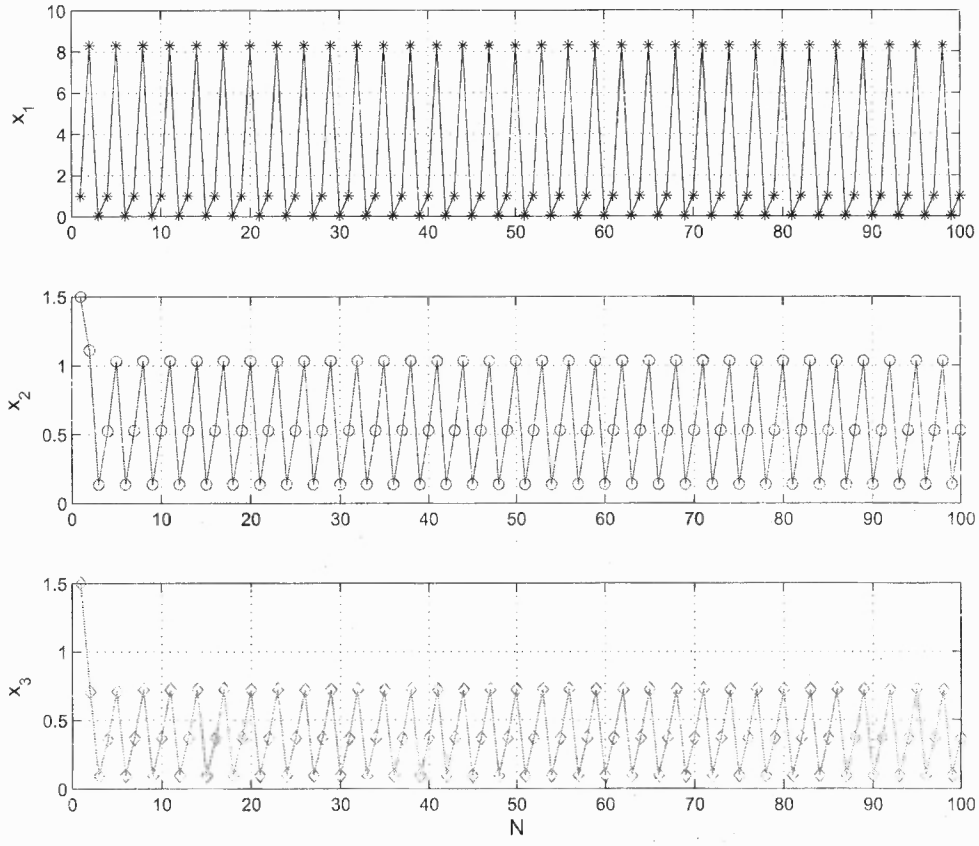

Figure 5.4 Time series plot for 3-dimensional all-pioneer hierarchical model showing period 3-cycle for the same parametric values as used in Figure 5.3.

Theorem 5.0.1. *System (5.2) has a stable 3-cycle for the following parameter ranges:*

$$2.9 < a < 3.3,\ 1.3 < b,\ c < 2,\ 0 \leq c_{ij} \leq 0.4$$

We shall sketch the proof in the following section.

5.1 Finding a Stable 3-Cycle For The All-Pioneer, Hierarchical System

$$\begin{aligned} x_1(n+1) &= x_1(n)e^{a-x_1(n)} \\ x_2(n+1) &= x_2(n)e^{b-\alpha x_1(n)-x_2(n)} \\ x_3(n+1) &= x_3(n)e^{c-\beta x_1(n)-\gamma x_2(n)-x_3(n)} \end{aligned} \tag{5.2}$$

where $a,\ b,\ c > 0$ and $\alpha,\ \beta,\ \gamma > 0$. Let us now briefly describe the proof of Theorem 5.0.1 First we find a superstable 3-cycle for $x \to f_1(x) := xe^{a-x}$.

Note $f_1(0) = 0$ and $f_1(x) \downarrow 0$ as $x \uparrow \infty$. The fixed points are $x = 0$ and $x = a$. To see if these are stable, we compute

$$f_1' = (1-x)e^{a-x}$$

Hence,

$f_1'(0) = e^a > 1 \ \Rightarrow$ 0 is an unstable fixed point

$f_1'(a) = (1-a) \ \Rightarrow \ x = a$ is stable if $0 < a < 2$ and unstable if $a > 2$

Let us find the maximum and maximizer (= point x at which the maximum is attained)

$$f_1' = (1-x)e^{a-x} = 0 \ \Rightarrow \ x = 1,$$

so the maximizer is $x = 1$ and the maximum is $f(1) = e^{a-1}$. A graph of f_1 is sketched in Figure 5.5 (for $a > 1$).

We now find an a having a superstable 3-cycle including the maximizer where $f_1' = 0$ ($\Rightarrow$ superstable). Such a cycle is illustrated with the cobweb map shown in

Figure 5.6. We see from the cobweb map that

$$x_{(0)} = 1 \rightarrow x_{(1)} := f_1(x_{(0)}) = e^{a-1} \rightarrow x_{(2)} := f_1(x_{(1)}) = e^{a-1}exp(a - e^{a-1})$$
$$\rightarrow x_{(0)} := f_1(x_{(2)}) = e^{a-1}exp(a - e^{a-1})exp[a - (e^{a-1}exp(a - e^{a-1}))]$$

Accordingly a must satisfy the equation

$$\Delta(a) := 3a - 1 - e^{a-1}[1 + exp(a - e^{a-1})] = 0 \tag{5.3}$$

Clearly, $a = 1$ is a solution, but this just produces a degenerate 3-cycle comprised only of the fixed point $x = a$. We seek another solution with $a = a_* > 2$. Note that a simple computation shows that

$$\Delta(3) = 8 - e^2[1 + exp(3 - e^2)] \cong 0.51923 > 0$$

and

$$\Delta(4) = 11 - e^3[1 + exp(4 - e^3)] \cong -9.08554 < 0$$

Thus the desired solution of (2) lies between 3 and 4. Using the bisection method [23] we find

$$a_* \cong 3.1176$$

We conclude then that $f(x) := xe^{a-x}$ has a superstable 3-cycle comprised of the points $\{1,\ e^{a_*-1},\ e^{a_*-1}exp(a_* - e^{a_*-1})\}$.

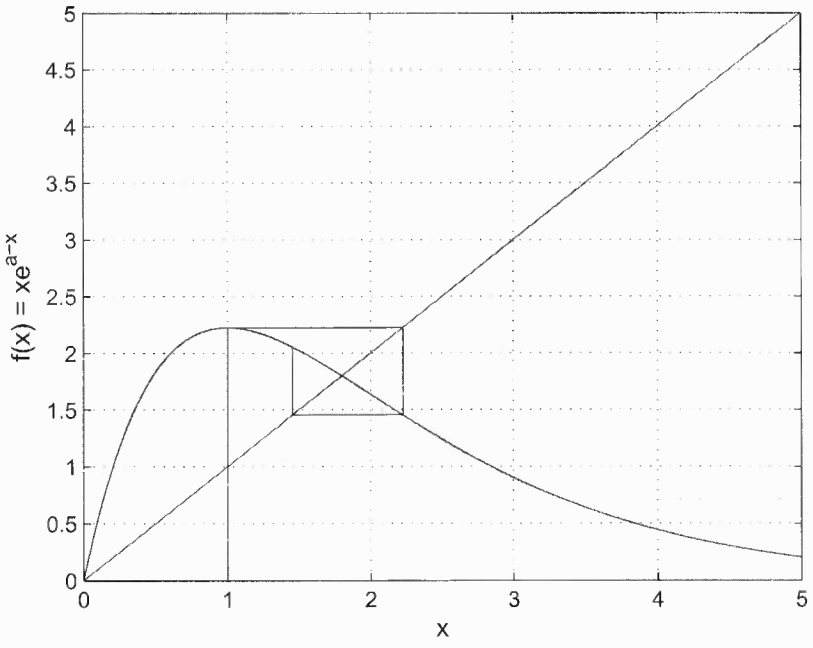

Figure 5.5 A cobweb map for pioneer species with the positive parameter $a = 1.8$.

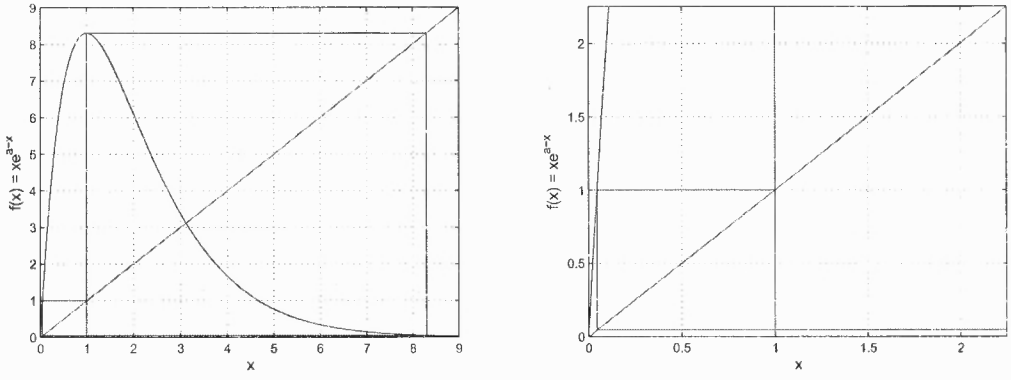

(a) A superstable 3-cycle.

(b) Zoomed version of Figure 5.6(a)

Figure 5.6 Cobweb map for pioneer species with parameters $a = 3.1167$ and $c_{11} = 1$.

Returning to the original system (5.1), let us first consider the case where, $\alpha,\ \beta,\ \gamma = 0$, so we have the uncoupled system

$$\begin{aligned} x_1(n+1) &= x_1(n)e^{a_*-x_1(n)} \\ x_2(n+1) &= x_2(n)e^{b-x_2(n)} \\ x_3(n+1) &= x_3(n)e^{c-x_3(n)} \end{aligned} \tag{5.4}$$

If we set $b = c = 1.5$, then it is clear from the above that

$$\{(1,\ b,\ c),\ (e^{a_*-1},\ b,\ c),\ (e^{a_*-1}exp(a_* - e^{a_*-1}),\ b,\ c)\}$$

is a stable 3-cycle of (5.4). However, we want some coupling, but we don't want to perturb this stable 3-cycle by much. Therefore, we consider the following special case of (5.1):

$$\begin{aligned} x_1(n+1) &= x_1(n)e^{a_*-x_1(n)} \\ x_2(n+1) &= x_2(n)e^{1.5-0.3x_1(n)-x_2(n)} \\ x_3(n+1) &= x_3(n)e^{1.5-0.3x_1(n)-0.3x_2(n)-x_3(n)} \end{aligned} \tag{5.5}$$

This can also be shown to have stable 3-cycle, a result that can be verified by numerical simulation, and proved along similar lines.

CHAPTER 6

BIFURCATION ANALYSIS

In a real world ecosystem, species tend not to behave the same way throughout their entire life spans. There are many changes continuously occurring in nature that affect the whole ecosystem. To explain such behavior of the species, we apply *bifurcation analysis*, which acts as a bridge between behavioral changes that species exhibit as some of the system parameters vary. Many types of such changes or bifurcations can be observed in numerical simulations, and they can actually be proved to occur for the discrete dynamical system models that we are considering. However, some of the more abundant types of bifurcations, such as the Hopf bifurcation, in which a fixed point becomes unstable (stable) and gives birth to a stable (unstable) periodic orbit of period greater than two [47] can actually be shown not to occur in our hierarchical models. In particular, one has the following result.

Lemma 6.0.2. *There are no Hopf bifurcations for our 3-dimensional discrete pioneer-climax hierarchical model.*

Proof. It suffices to prove this result for the all climax case, since the proof for any combination of climax and pioneer components is completely analogous. The all-climax 3-dimensional hierarchical model has the form:

$$\begin{aligned} x_1(n+1) &= x_1(n)(c_{11}x_1(n))e^{a-c_{11}x_1(n)} \\ x_2(n+1) &= x_2(n)(c_{21}x_1(n)+c_{22}x_2(n))e^{b-c_{21}x_1(n)-c_{22}x_2(n)} \\ x_3(n+1) &= x_3(n)(c_{31}x_1(n)+c_{32}x_2(n)+c_{33}x_3(n))e^{c-c_{31}x_1(n)-c_{32}x_2(n)-c_{33}x_3(n)} \end{aligned} \tag{6.1}$$

Denoting $\mathbf{1} := (1,1,1)$, and all the other system parameters by $\boldsymbol{\mu} := (a, b, c, c_{11}, \cdots, c_{33})$ we have

$$T_{\mathbf{1},\,\boldsymbol{\mu}}(x_1(n), x_2(n), x_3(n)) := (x_1(n+1), x_2(n+1), x_3(n+1)).$$

The Jacobian $J = T'_{1,\,\mu}$ at any point is:

$$J = \begin{bmatrix} A(2xc_{11} - c_{11}^2x^2) & 0 & 0 \\ B(yc_{21} - yc_{21}(xc_{21} + yc_{22})) & B(xc_{21} + yc_{22} - yc_{22}(xc_{21} + yc_{22})) & 0 \\ C(zc_{31} - z(xc_{31} + yc_{32} + zc_{33}c_{31})) & C(zc_{32} - zc_{32}(xc_{31} + yc_{32} + zc_{33})) & C(xc_{31} + yc_{32} + zc_{33} + D) \end{bmatrix} \tag{6.2}$$

where,

$$A = e^{a - c_{11}x}$$

$$B = e^{b - c_{21}x - c_{22}y}$$

$$C = e^{c - c_{31}x - c_{32}y - c_{33}z}$$

$$D = zc_{33} - zc_{33}(xc_{31} + yc_{32} + zc_{33})$$

As observed above, the eigenvalues are simply the diagonal elements, and these are obviously real numbers. Therefore, we cannot have complex eigenvalues, which is a necessary condition for the existence of a Hopf bifurcation. □

We note that it is not difficult to show that Hopf bifurcations are possible if the system is not hierarchical [47].

6.1 Period-Doubling Bifurcation

In light of the above lemma, we now proceed to find some other types of bifurcation, which can play significant roles in dynamical population models. The phenomenon of a period-doubling bifurcation (or flip bifurcation) occurs in many discrete dynamical systems, and we expect it to occur in our model based upon numerous numerical simulations and experimental evidence. In period-doubling bifurcation, a fixed point becomes unstable (stable) and creates a stable (unstable) 2-cycle. Well-known criteria for such bifurcations are given in the following result [50]

Theorem 6.1.1. *The following are sufficient conditions for occurrence of period-doubling bifurcation in a 1-parameter family of $C^r (r \geq 3)$ 1-dimensional maps*

$$x(k+1) = f(x(k),\ \mu), \quad x \in \mathbb{R}^1, \quad \mu \in \mathbb{R}^1,\ k \geq 0.$$

1. $f(x^*,\ \mu^*) = x^*$,
2. $f_x(x^*,\ \mu^*) = -1$,
3. $f^2_\mu(x^*,\ \mu^*) = 0$,
4. $f^2_{xx}(x^*,\ \mu^*) = 0$,
5. $f^2_{x\mu}(x^*,\ \mu^*) \neq 0$,
6. $f^2_{xxx}(x^*,\ \mu^*) \neq 0$, *where, x^* is the fixed point and μ^* is the bifurcation value.*

As we noted earlier, bifurcations of the period-doubling or flip type tend to be the most prevalent for our hierarchical pioneer-climax system. We shall now study flip bifurcations in detail: starting with the one-dimensional model and then generalizing the result to the three-dimensional case in a step-by-step manner.

We begin by considering one-dimensional pioneer and climax maps represented in the form $f : \mathbf{R}_+ \to \mathbf{R}_+$, where

$$f(x) = f(x; a,\ c) := xe^{a - c_{11}x} \tag{6.3}$$

and

$$g(x) = g(x; a,\ c) := x^2 c_{11} e^{a - c_{11}x} \tag{6.4}$$

respectively where a is a positive parameter that we vary, and the intra-species interaction parameter c_{11} is a positive, fixed quantity. For our analysis of flip bifurcations, we could use Theorem 6.1.1, but we shall find it more convenient to provide direct proofs that take full advantage of the special forms of the maps (6.3) and (6.4).

First, we shall characterize the fixed points of the two functions.

Lemma 6.1.2. *The map f given by 6.3 has precisely two fixed points: $x = 0$ and $x = a/c_{11}$, with $f'(0) = e^a$ and $f'(a/c_{11}) = 1 - a$, so the origin is always unstable, and a/c_{11} is stable (unstable) if $|1 - a|$ is less than (greater than) one. On the other hand, g always has 0 as a superstable fixed point, and this is the only fixed point if $a < 1 + ln(c_{11})$. If $a = 1 + ln(c_{11})$, g also has the fixed point $x = 1$, with $g'(1) = 1$ which is unstable from the left, but stable from the right. If $a > 1 + ln(c_{11})$, g has the superstable fixed point 0, and an unstable fixed point at the smaller of the two positive solutions x_l of*

$$xc_{11}e^{a-c_{11}x} = 1 \tag{6.5}$$

for which $0 < x_l < 1$, and another fixed point x_r at the larger of the two solutions ($x_r > 1$), which is stable or unstable according as the absolute value of $g'(x_r) = x_r c_{11}(2 - c_{11}x_r)e^{a-c_{11}x_r}$ is less than or greater than one, respectively.

Proof. As the solutions of

$$f(x) = xe^{a-c_{11}x} = x, \tag{6.6}$$

are obviously $x = 0$ and $x = a/c_{11}$, these are the fixed points of f. The stability results for these fixed points of f follows from the formula for the derivative

$$f'(x) = (1 - c_{11}x)e^{a-c_{11}x} \tag{6.7}$$

The fixed points of g are the nonnegative solutions of

$$g(x) = x^2 c_{11}e^{a-c_{11}x} = x, \tag{6.8}$$

so $x = 0$ is always a solution. For positive solutions, we can divide the above by x to obtain

$$h(x) := xe^{a-c_{11}x} = 1, \tag{6.9}$$

A simple calculation shows that the maximum of h is $\frac{e^{a-1}}{c}$, which occurs at $x = 1$. The remaining results concerning the positive fixed points of g follow from this formula, the derivative

$$g'(x) = c_{11}x(2 - c_{11}x)e^{a-c_{11}x} \tag{6.10}$$

and a simple cobweb argument for the fixed point x_l, so the proof is complete. □

A necessary condition for a flip bifurcation to occur at a fixed point is that the derivative be equal to -1. Relevant to this is our next result, which follows directly from Lemma 6.1.2 and the above proof. We leave the elementary proof to the reader.

Lemma 6.1.3. *The fixed point a/c_{11} is stable for $0 < a < 2$, $f'(a/c_{11}) = -1$ at $a = 2$, and decreases thereafter, so a/c_{11} is unstable for $a > 2$. The derivative $g'(x_r)$ is a decreasing function of a, starting at $g'(x_r) = 1$ when $a = 1 + ln(c_{11})$ and $x_l = x_r$, and $g'(x_r) \to -\infty$ as $a \to \infty$. Consequently, there is a unique value of $a > 1 + ln(c_{11})$ where $g'(x_r) = -1$; namely, $x_r = 3/c_{11}$, which corresponds to $a = 3 + ln(c/3)$.*

We next prove that a supercritical flip bifurcation occurs at the fixed points of f and g at which derivatives are equal to -1. Recall that by supercritical we mean that a fixed point transitions from stable to unstable across the bifurcation value of a, and gives birth to a stable 2-cycle.

Theorem 6.1.4. *Both the pioneer map $f(x) = xe^{a-c_{11}x}$ and the climax map $g(x) = x^2c_{11}e^{a-c_{11}x}$ have supercritical flip bifurcations at their largest fixed points given by $x_1 = a/c_{11}$ and $x_2 = 3/c_{11}$, respectively, when $f'(x_1) = -1$ and $g'(x_2) = -1$ for $a = 2$ and $a = 3 + ln(c_{11}/3)$.*

Proof. We give the proof only for the pioneer case since the argument for the climax function is completely analogous (although admittedly rather more complicated). For simplicity, we assume $c_{11} = 1$, which does not really affect the method of proof. Thus, we deal with the bifurcation at the fixed point $x = a$ of $f(x) = xe^{a-x}$ as the parameter crosses $a = 2$.

To show the flip bifurcation, we study f and f^2, where

$$f^2(x) := f(f(x)) = (xe^{a-x})exp(a - xe^{a-x})$$

for $a > 2$. Of course, as $x = a$ is a fixed point of f, it is also a fixed point of f^2. It follows from Lemma 6.1.3 that f has a unique fixed point in a neighborhood of $x = a$, and $x = a$ is an unstable fixed point of f for $a > 2$; therefore, it is also an unstable fixed point of f^2 since $f^{2'}(a) = (f'(a))^2 > 1$ for $a > 2$. We now show that f^2 has additional fixed points $x_*^{(-)} < \hat{x} = 2 + \mu < x_*^{(+)}$ when μ is a sufficiently small positive number such that $x_*^{(-)}$, $x_*^{(+)} \to 2$ as $\mu \to 0$. Clearly, this implies that $\{x_*^{(-)}, x_*^{(+)}\} = \{x_*^{(-)}, f(x_*^{(-)})\} = \{f(x_*^{(+)}), x_*^{(+)}\}$ is a 2-cycle of f. The fixed points of f^2 near $x = a$, satisfy

$$xe^{a-x}exp(a - xe^{a-x}) = x,$$

and since $x \neq 0$, this is equivalent to

$$exp[2a - x(1 + e^{a-x})] = 1,$$

which holds iff

$$2a - x(1 + e^{a-x}) = 0 \tag{6.11}$$

It is easy to see that $x = a$ is a solution of (6.11) for every $a > 0$. Let us now consider this equation with $a = 2 + \mu$ for small nonnegative values of μ, so that

if $x = a + y = 2 + \mu + y$, we have

$$\psi(y) = \psi(y;\ \mu) := 2(2+\mu) - [(2+\mu) + y][1 + e^{-y}] = 0 \tag{6.12}$$

Clearly $y = 0$ is a solution of (6.12) for every $\mu \geq 0$, and this corresponds to the fixed point $x = \hat{x} = a$ of f. But, there are two other solutions that comprise a (nontrivial) 2-cycle of f.

Noting that $\psi(0;\ \mu) = 0$ for all $\mu \geq 0$, $\psi \to -\infty$ as $y \to +\infty$, $\psi \to +\infty$ as $y \to -\infty$, $\frac{d\psi}{dy}(0;\ \mu) = \mu$, and performing a more detailed curve plotting analysis, we find that graph of ψ has the form shown below for $\mu > 0$.

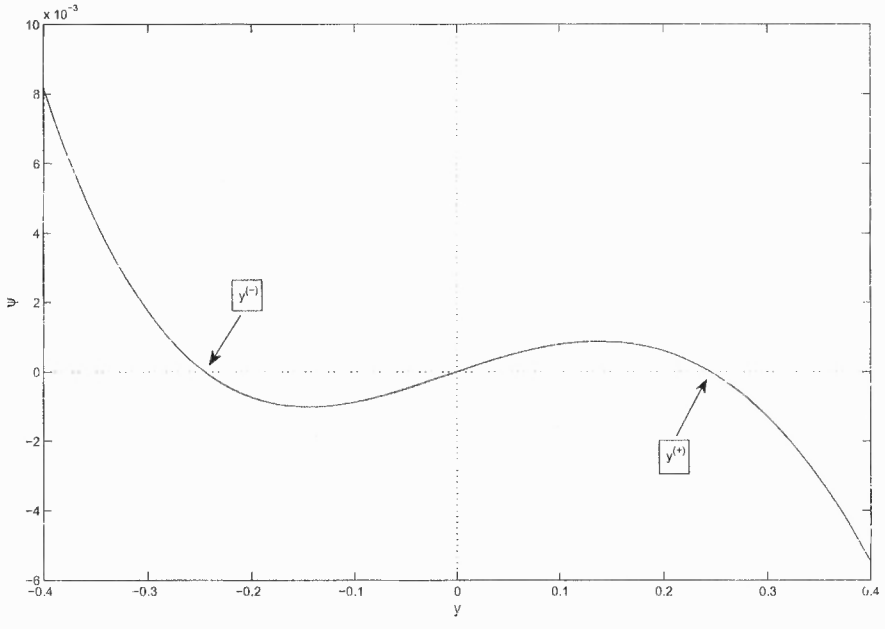

Figure 6.1 ψ as a function of y for $\mu = 0.01$

Accordingly it has a positive and negative zero $y^{(+)} = y^{(+)}(\mu)$ and $y^{(-)} = y^{(-)}(\mu)$, respectively, for every sufficiently small positive value of the parameter μ. To

find the nature of these zeros, we assume series solutions of the form

$$y^{(-)} = \sum_{k=1}^{\infty} a_k^{(-)} \sigma^k, \; y^{(+)} = \sum_{k=1}^{\infty} a_k^{(+)} \sigma^k,$$

where $\sigma = \sqrt{\mu}(\mu \geq 0)$. We then substitute these series in (6.12), wherein we use the expansion $e^{-y} = \sum_{k=0}^{\infty} \frac{(-1)^k y}{k!}$, to obtain

$$\psi = 2(2+\sigma^2) - [(2+\sigma^2)+y][2+\sum_{k=0}^{\infty} \frac{(-1)^k y^k}{k!}] = 0$$

$$\Longrightarrow \quad -\sigma^2 + \frac{\sigma^2 y}{2} + \frac{1}{3!}(1-\sigma^2)y^2 + \frac{1}{4!}(1-\sigma^2)y^3 + \cdots = 0$$

$$\Longrightarrow \quad -\sigma^2 + \frac{\sigma^2}{2}\sigma\left(\sum_{k=1}^{\infty} a_k \sigma^{k-1}\right) + \frac{1}{3!}(1-\sigma^2)\sigma^2\left(\sum_{k=1}^{\infty} a_k \sigma^{k-1}\right)^2$$
$$+\frac{1}{4!}(1-\sigma^2)\sigma^2\sigma\left(\sum_{k=1}^{\infty} a_k \sigma^{k-1}\right)^3 + \cdots = 0$$

$$\Longrightarrow \quad -1 + \frac{1}{2}\sigma\left(\sum_{k=1}^{\infty} a_k \sigma^{k-1}\right) + \frac{1}{3!}(1-\sigma^2)\left(\sum_{k=1}^{\infty} a_k \sigma^{k-1}\right)^2$$
$$+\frac{1}{4!}(1-\sigma^2)\sigma\left(\sum_{k=1}^{\infty} a_k \sigma^{k-1}\right)^3 + \cdots = 0,$$

which can be solved recursively to yield $a_1 = \pm\sqrt{6}$, $a_2 = -\frac{9}{4}$, $\cdots$ etc. So, we see that $y^{(-)}$, $y^{(+)}$ are analytic in $\sqrt{\mu}$ for $\mu \geq 0$ sufficiently small, and

$$y^{(-)} = -\sqrt{\mu}\left[\sqrt{6} + \frac{9\mu}{4} + O(\sqrt{\mu})\right],$$
$$y^{(+)} = \sqrt{\mu}\left[\sqrt{6} - \frac{9\mu}{4} + O(\sqrt{\mu})\right] \text{ as } \mu \downarrow 0$$

Therefore, in addition to the fixed point $\hat{x} = 2 = 2 + \mu$ of f, f^2 has another pair of fixed points $x_*^{(-)} = 2 - \sqrt{6\mu} + O(\mu) < \hat{x} < x_*^{(+)} = 2 + \sqrt{6\mu} + O(\mu)$ for sufficiently small $\mu \geq 0$. Hence, $\{x_*^{(-)}, x_*^{(+)}\}$ is a (nontrivial) 2-cycle for f for sufficiently small positive μ, and this is stable since it is easy to verify that $|f^{2'}(x_*^{(-)})| = |f'(x_*^{(-)})f'(x_*^{(+)})| < 1$ for $\mu > 0$ sufficiently small. Thus the proof is complete. □

6.2 Codimension - One Flip Bifurcations

We now use the above results to show that if any of the parameters a, b or c varies, while the other two are fixed, the whole system exhibits a supercritical flip bifurcation. The dynamics of our discrete hierarchical system is determined by the iterates of the map $T : \mathbf{R}^3_+ \to \mathbf{R}^3_+$ defined as

$$T(x) = T(x_1,\ x_2,\ x_3) = (f_1(x_1;\ a),\ f(x_1,\ x_2;\ b),\ f_3(x_1,\ x_2,\ x_3;\ c))$$

where f_1, f_2, f_3 are either pioneer or climax type functions, and we have indicated only the dependence on the positive parameters a, b and since we are assuming that only they, and not the interaction coefficients c_{ij} are allowed to vary.

Recall that the derivative matrix of T at any point can be represented by the triangular jacobian matrix

$$T'(x) = \begin{pmatrix} \frac{\partial f_1}{\partial x_1} & 0 & 0 \\ \frac{\partial f_2}{\partial x_1} & \frac{\partial f_2}{\partial x_2} & 0 \\ \frac{\partial f_3}{\partial x_1} & \frac{\partial f_3}{\partial x_2} & \frac{\partial f_3}{\partial x_3} \end{pmatrix} \tag{6.13}$$

with eigenvalues $\lambda_1 = \frac{\partial f_1}{\partial x_1}(x)$, $\lambda_2 = \frac{\partial f_2}{\partial x_2}(x)$, $\lambda_3 = \frac{\partial f_3}{\partial x_3}(x)$ that may be viewed as associated with the parameters a, b and c respectively. Our codimension-one generalization of Theorem 6.1.4 is the following result:

Theorem 6.2.1. *Let one of the three eigenvalues be equal to -1 and the other two eigenvalues be less than one in absolute value at a fixed point of T. Let $v = a$, b or c be the parameter associated with eigenvalue equal to -1. Then there is a bifurcation value v_* and corresponding fixed point $\hat{x}$ of T giving rise to a supercritical flip bifurcation.*

Proof. For simplicity, we consider only the all pioneer case

$$\begin{aligned} T(x) &= (f_1(x_1;\ a),\ f_2(x_1,\ x_2; b),\ f_3(x_1,\ x_2,\ x_3;\ c)) \\ &= (x_1 e^{a-x_1},\ x_2 e^{b-x_1-x_2},\ x_3 e^{c-x_1-x_2-x_3}), \end{aligned} \tag{6.14}$$

where we have set all the interaction coefficients equal to unity. There is no real loss of generality in restricting our demonstration in this way, because the result in the completely general setting is proved using the same approach with the obvious modifications.

The fixed point in question must be $\hat{x} = (a,\ b-a,\ c-b)$. If it is λ_1 that equals -1, with associated $v = a$, the proof follows directly from the one-dimensional result in Theorem 6.1.4. If $\lambda_2 = -1$, or $\lambda_3 = -1$ with associated parameters b or c, respectively, the proof is only slightly more difficult. We consider only $\lambda_2 = -1$, since the proof for $\lambda_3 = -1$ is essentially the same. In this case, we see from (6.13) and (6.14) that the eigenvalues of $T'(\hat{x})$ are $-1 < \lambda_1 = 1-a < 1$, $\lambda_2 = 1-(b-a) = -1$ and $-1 < \lambda_3 = 1-(c-b) < 1$. Now we fix a and vary b slightly while keeping c fixed and maintaining $-1 < 1-(c-b) < 1$. Observe that

$$\begin{aligned} T^2(x) &= T(T(x)) \\ &= (f_1(f_1(x_1)),\ f_2(f_1(x_1),\ f_2(x_1,\ x_2)),\ f_3(f_1(x_1), f_2(x_1,x_2), f_3(x_1,x_2,x_3))) \\ &= (x_1 exp[2a - x_1(1+e^{a-x_1})],\ x_2 exp[2b - x_1(1+e^{a-x_1}) - x_2(1+e^{b-x_1-x_2})], \\ &\quad x_3 exp[2c - x_1(1+e^{a-x_1}) - x_2(1+e^{b-x_1-x_2}) - x_3(1+e^{c-x_1-x_2-x_3})]) \end{aligned} \tag{6.15}$$

and it is easy to see that $T^2(\hat{x}) = T^2(a,\ b-a,\ c-b) = \hat{x}$, so naturally $\hat{x}$ is also a fixed point of T^2. To find the bifurcation in the x_2 coordinate, we set $v = b = a+2+\mu = v_* + \mu$ and $x_2 = (b-a) + y_2 = 2 + \mu + y_2$. We want to find fixed points $x_* = \hat{x} + (0,\ y_2,\ y_3)$ of T^2 near $\hat{x}$ for sufficiently small $\mu \geq 0$. It follows from (6.15) that x_* must satisfy the equations

$$\begin{aligned} 2(2+\mu) - (2+\mu+y_2)(1+e^{-y_2}) &= 0 \\ 2(c-a) - (b-a+y_2)(1+e^{-y_2}) - (c-b+y_3)(1+e^{-y_2-y_3}) &= 0 \end{aligned} \tag{6.16}$$

We see from the proof of Theorem 1 that the first of the above equations has in addition to $y_2 = 0$ a pair of nonzero solutions $y_2^{(-)} = -\sqrt{6\mu} + O(\mu) \leq 0 \leq y_2^{(+)} =$

$\sqrt{6\mu} + O(\mu)$ for all sufficiently small $\mu \geq 0$. Upon substituting either of these in the second of equations (6.16), and taking note of the first equation, we obtain

$$\psi(y_3,\ \mu) := 2(c-b) - (c-b+y_3)(1 + e^{-y_2^{(\pm)}(\sqrt{\mu})-y_3}) = 0 \tag{6.17}$$

We compute that $\frac{d\psi}{dy_3}(0,\ \mu) = -1 + [(c-b) - 1]e^{-y_2^{(\pm)}(\sqrt{\mu})}$, whereupon it follows from $-1 < \lambda_3 = 1 - (c-b) < 1$ that this derivative is not zero for all sufficiently small μ. Hence, we infer from the implicit function theorem that (6.17) has a unique solution $y_3^{(\pm)} = y_3^{(\pm)}(\mu)$ going to zero with μ, and $y_3(\mu)$ is actually a smooth function of $y_2(\mu)$, which is a smooth function of $\sqrt{\mu}$. Collecting all of the above properties, we see that

$$x_*^{(+)} = (a,\ b-a+y_2^{(+)},\ c-b+y_3^{(+)})$$
$$x_*^{(-)} = T(x_*^{(+)}) = (a,\ b-a+y_2^{(-)}, c-b+y_3^{(-)})$$

is a 2-cycle of T in a neighborhood of the fixed point $\hat{x} = (a,\ b-a,\ c-b)$ for $b = a+2+\mu$ varying and the parameters a and c fixed. In addition, it is straightforward to show that $||\hat{x} - x_*|| = O(\sqrt{\mu})$ and that the eigenvalues of $T^{2'}(x_*^{(-)})$ = eigenvalues of $T^{2'}(x_*^{(+)})$ all have absolute value less than 1, so $\{x_*,\ T(x_*)\}$ is a stable 2-cycle. As it is clear that the fixed point x_* is unstable (in the x_2 direction) for all $\mu > 0$, the proof is complete. □

6.3 Codimension - Two Flip Bifurcations

Let us consider the case where two of the parameters a, b and c are varied- say along a curve in one of the parameter planes passing through a point where two of the eigenvalues of (6.13) are equal -1, while the remaining eigenvalues is of absolute value less than one. A natural question to ask for this codimension-2 parameter variation is, what are the properties of any flip bifurcations that may occur?

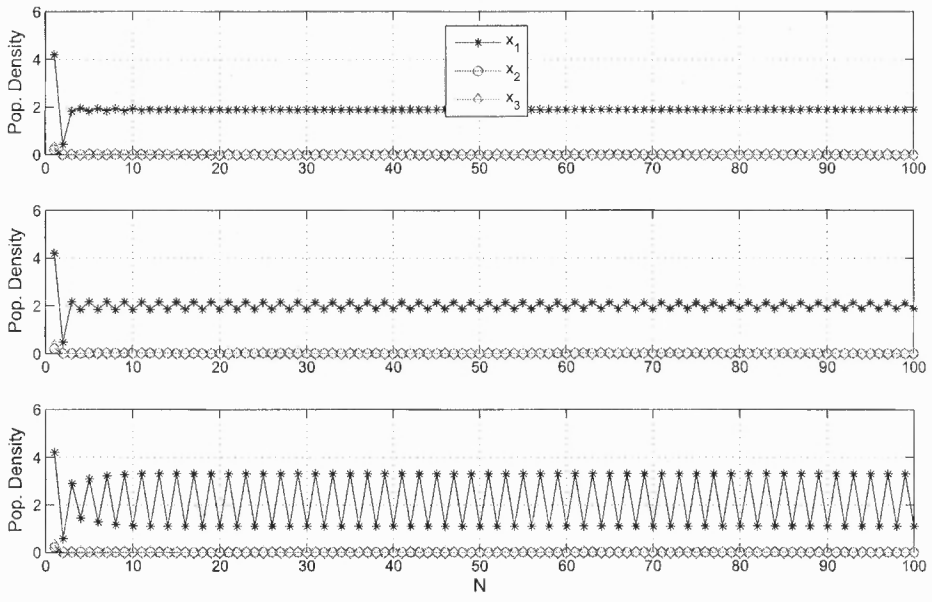

Figure 6.2 The phenomenon of codimension - one period doubling, when all the species are pioneer. Here the bifurcation parameter is $a = 2$.

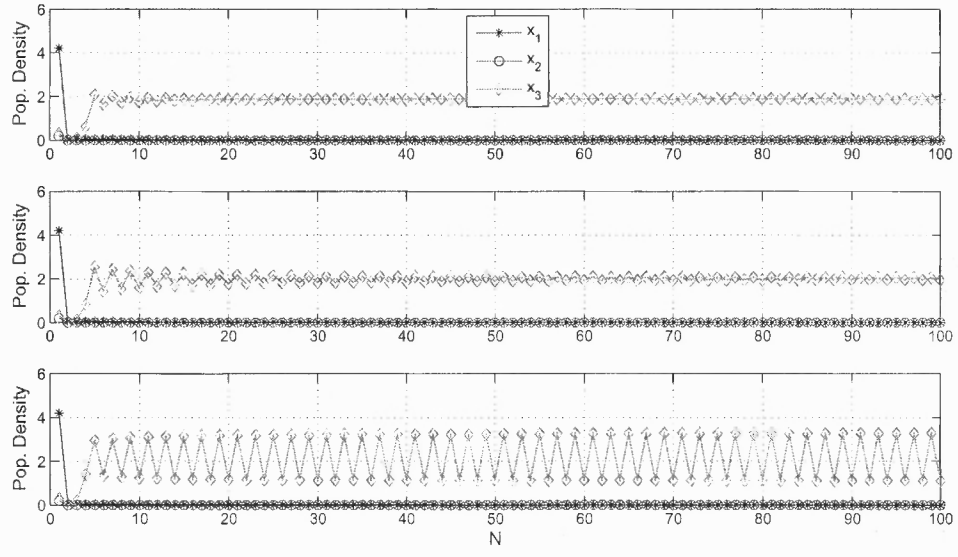

Figure 6.3 The phenomenon of codimension - one period doubling, when all the species are pioneer. Here the bifurcation parameter is $c = 2$.

To see what flip possibilities there may be, it is instructive to first investigate the simple, uncoupled all-pioneer map

$$P(x_1,\ x_2,\ x_3) = (x_1 e^{a-x_1},\ x_2 e^{b-x_2},\ x_3 e^{c-x_3}) \tag{6.18}$$

with $a = b = 2$ and $0 < c < 2$. Let us fix c and vary a and b along the curve $b - a = 0$ in the a, b-plane, concentrating on a neighborhood of $(a,\ b) = (2,\ 2)$ in this plane. Owing to the fact that the system is uncoupled, Theorem 1 applied to each coordinate function yields the following characterization of the flip bifurcations at $x_* = (a = 2,\ b = 2,\ c)$: As a and b cross the value 2 in an increasing fashion along any smooth curve in the a, b-plane passing through $(2,\ 2)$, flip bifurcations occur. These bifurcations can be described as follows: In addition to the trivial, unstable 2-cycle at $(a,\ b,\ c)$ we have

1. There are a pair of (nontrivial) stable 2-cycles; namely $\{(a+y_1^{(-)},\ b+y_2^{(-)},\ c),\ (a+y_1^{(+)},\ b+y_1^{(+)},\ c)\}$ and $\{(a+y_1^{(-)},\ b+y_2^{(+)},\ c),\ (a+y_1^{(+)},\ b+y_1^{(-)},\ c)\}$.

2. There are also two (nontrivial) stable 2-cycles; namely $\{(a+y_1^{(-)},\ b,\ c),\ (a+y_1^{(+)},\ b,\ c)\}$ and $\{(a,\ b+y_2^{(-)},\ c),\ (a,\ b+y_1^{(-)},\ c)\}$,

and in all cases the fixed point $(a,\ b,\ c)$ changes from an attractor to a repeller upon such a crossing of $(2,\ 2)$ in the a, b-plane.

As one might expect, our general hierarchical 3-dimensional system has analogous qualitative, codimension-2 flip bifurcation behavior. We summarize this in the following:

Theorem 6.3.1. *Suppose that two of the eigenvalues of (6.13) at a fixed point $\hat{x}$ are equal to -1, while the remaining eigenvalue is less than one in absolute value. Let the parameters associated with the eigenvalues equal to -1 be varied across a smooth curve through the point in their coordinate plane so as to simultaneously increase the two parameters. Then just as in the uncoupled case above, in a neighborhood of the fixed point $\hat{x}$, $\hat{x}$ changes from an attractor to a repeller as the parameters pass through the*

bifurcation point, giving birth to four (nontrivial) 2-cycles; two of which are stable, while the other two are unstable.

Proof. Once again, we shall give the proof only for the all-pioneer system (6.14), and here we shall only consider the case where $\lambda_1 = 1 - a = \lambda_2 = 1 - (b - a) = -1$, and $-1 < \lambda_3 = 1 - (c - b) < 1$. A proof for the most general case, which we leave to the reader can be based on the argument that follows, with only minor modifications.

We simply extend the methods of proof of Theorems 1 and 2. Denote the fixed point of T as $\hat{x} := (a,\ b-a,\ c-b)$, and set $a = 2 + \mu$ and $b = a + 2 + \nu = 4 + \mu + \nu$, where $\mu,\ \nu \geq 0$ are sufficiently small. Define $x_* = \hat{x} + (y_1,\ y_2,\ y_3) = (2 + \mu + \nu,\ 2 + \nu + y_2,\ c - (4 + \mu + \nu) + y_3)$, which denotes solutions of $T^2(x_*) = x_*$ for $\mu, \nu \geq 0$ sufficiently small, and the $y_1,\ y_2,\ y_3$ are correspondingly small coordinate increments. Following obvious extensions of the arguments in the proof of Theorems 1 and 2, it is easy to see that the increments must satisfy the following system of equations:

$$\begin{aligned} 2(2+\mu) - [(2+\mu)+y_1][1+e^{-y_1}] &= 0, \\ 2(4+\mu+\nu) - [(2+\mu)+y_1][1+e^{-y_1}] - [(2+\nu)+y_2][1+e^{-y_1-y_2}] &= 0, \\ 2c - [(2+\mu)y_1][1+e^{-y_1}] - [(2+\nu)+y_2][1+e^{-y_1-y_2}] & \\ -[(c-4-\mu-\nu)+y_3][1+e^{-y_1-y_2-y_3}] &= 0. \end{aligned} \tag{6.19}$$

Evidently $y_1 = y_2 = y_3 = 0$ is a solution of (6.19) for all $\mu,\ \nu \geq 0$, and this corresponds to $\hat{x}$, which is a fixed point of T and therefore trivially a fixed point of T^2. It remains to find the nontrivial fixed points of T^2 near $\hat{x}$, which generate nontrivial 2-cycles of T for sufficiently small $\mu, \nu \geq 0$. We infer from Theorem 1 that along with $y_1 = 0$, there is pair of solutions $y_1^{(\pm)} = \phi^{(\pm)}(\sqrt{\mu}) = \pm\sqrt{6\mu} + O(\mu)$, where $\phi^{(\pm)}$ are analytic functions for sufficiently small $\mu \geq 0$. We now proceed to the second of equations (6.19) for each of $y_1 = 0,\ \phi^{(-)}(\sqrt{\mu})$ and $\phi^{(+)}(\sqrt{\mu})$.

Substituting $y_1 = 0$ in the second equation of (6.19) yields

$$2(2+\nu) - [(2+\nu) + y_2][1 + e^{-y_2}] = 0 \tag{6.20}$$

Noting the similarity of (6.20) to the first equation of (6.19), it is clear that for $y_1 = 0$, the second equation of (6.19) has solutions $y_2 = 0$ and $y_2 = \phi^{(\pm)}(\sqrt{\nu})$ for all sufficiently small nonnegative ν.

On the other hand, substituting $y_1 = \phi^{(\pm)}(\sqrt{\mu})$ in the second equation of (6.19) and using the fact that $\phi^{(\pm)}(\sqrt{\mu})$ are solutions of the first of equations (6.19), we readily compute that

$$2(2+\nu) - [(2+\nu) + y_2][1 + e^{-\phi^{(\pm)}(\sqrt{\mu})-y_2}] = 0 \tag{6.21}$$

Then again applying our approach in the proof of Theorem 1, we find that for each of $\phi^{(-)}(\sqrt{\mu})$ and $\phi^{(+)}(\sqrt{\mu})$ there are three solutions; namely, $y_2 = \eta^{(-)}_{(+)}(\sqrt{\mu},\ \sqrt{\nu})$, $\eta^{(0)}_{(+)}(\sqrt{\mu},\ \sqrt{\nu}), \eta^{(+)}_{(+)}(\sqrt{\mu},\ \sqrt{\nu})$ for $y_1 = \phi^{(+)}(\sqrt{\mu})$ and $y_2 = \eta^{(-)}_{(-)}(\sqrt{\mu},\ \sqrt{\nu})$, $\eta^{(0)}_{(-)}(\sqrt{\mu},\ \sqrt{\nu})$, $\eta^{(+)}_{(-)}(\sqrt{\mu},\ \sqrt{\nu})$ for $y_1^{(+)} = \phi^{(-)}(\sqrt{\mu})$. These solutions satisfy the following readily verified properties: all of the functions are analytic for sufficiently small $\mu,\ \nu \geq 0$,

$$\begin{aligned}\eta^{(-)}_{(-)}(\sqrt{\mu},\ \sqrt{\nu}) < \phi^{(-)}(\sqrt{\nu}) < \eta^{(-)}_{(+)}(\sqrt{\mu},\ \sqrt{\nu}) < \eta^{(0)}_{(-)}(\sqrt{\mu},\ \sqrt{\nu}) < 0 < \\ \eta^{(0)}_{(+)}(\sqrt{\mu},\ \sqrt{\nu}) < \eta^{(+)}_{(+)}(\sqrt{\mu},\ \sqrt{\nu}) < \phi^{(+)}(\sqrt{\nu}) < \eta^{(+)}_{(-)}(\sqrt{\mu},\ \sqrt{\nu})\end{aligned} \tag{6.22}$$

for all sufficiently small $\mu,\ \nu > 0$, and $\eta^{(0,\ \pm)}_{(\pm)} = O(\sqrt{\mu},\ \sqrt{\nu})$ as $\mu,\ \nu \downarrow 0$.

To summarize our analysis so far, we have found that the first two equations of (15) have the following nine solutions for sufficiently small nonnegative values of the parameters μ and ν: (i) $y_1 = y_2 = 0$; (ii) $y_1 = 0,\ y_2 = \phi^{(+)}(\sqrt{\nu})$; (iii) $y_1 = 0,\ y_2 = \phi^{(-)}(\sqrt{\nu})$; (iv) $y_1 = \phi^{(+)}(\sqrt{\mu}),\ y_2 = \eta^{(0)}_{(+)}(\sqrt{\mu},\ \sqrt{\nu})$; (v) $y_1 = \phi^{(+)}(\sqrt{\mu}),\ y_2 = \eta^{(+)}_{(+)}(\sqrt{\mu},\ \sqrt{\nu})$; (vi) $y_1 = \phi^{(+)}(\sqrt{\mu}),\ y_2 = \eta^{(-)}_{(+)}(\sqrt{\mu},\ \sqrt{\nu})$; (vii) $y_1 = \phi^{(-)}(\sqrt{\mu}),\ y_2 = \eta^{(0)}_{(-)}(\sqrt{\mu},\ \sqrt{\nu})$; (viii) $y_1 = \phi^{(-)}(\sqrt{\mu}), y_2 = \eta^{(+)}_{(-)}(\sqrt{\mu}, \sqrt{\nu})$; and (ix) $y_1 = \phi^{(-)}(\sqrt{\mu}),\ y_2 =$

$\eta_{(-)}^{(-)}(\sqrt{\mu},\ \sqrt{\nu})$. It remains to solve the last equation of (6.19), where each of these nine solutions for the first two variables is substituted; this yields

$$\psi(y_3;\ \mu,\ \nu) := 2(c-b) - [(c-b)+y_3][1+e^{-y_1(\sqrt{\mu},\ \sqrt{\nu})-y_2(\sqrt{\mu},\ \sqrt{\nu})-y_3}] = 0 \qquad (6.23)$$

where $y_1 = y_1(\sqrt{\mu},\ \sqrt{\nu})$, $y_2 = y_2(\sqrt{\mu},\ \sqrt{\nu})$ are known analytic functions of $(\sqrt{\mu},\ \sqrt{\nu})$ for sufficiently small $\mu,\ \nu \geq 0$ given in turn by each of the solutions (i)-(ix) of the first two equations.

Now it follows from our assumption $|1-(c-b)| < 1$ that the same is true for all sufficiently small $\mu,\ \nu \geq 0$ in (6.23), which implies that

$$\frac{d\psi}{dy_3}(0;\ \mu,\ \nu) \neq 0, \qquad (6.24)$$

and this completes the proof. □

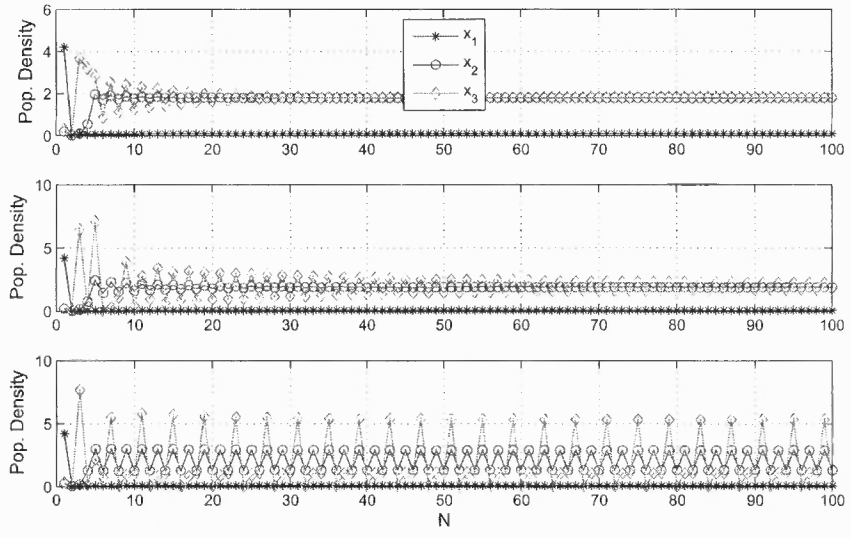

Figure 6.4 The phenomenon of codimension - two period doubling, when all the species are pioneer. Here the bifurcation parameters are b, and c are equal to 4 and 2, respectively.

6.4 Codimension - Three Flip Bifurcations

To complete our analysis of flip bifurcations, we consider the case where a, b and c are simultaneously varied past values where all of the eigenvalues of (6.13) are equal to -1. Again we take our cue from the uncoupled, all pioneer system (6.18). This time with $a = b = c = 2$, and a, b and c simultaneously exceeding 2 along some curve in a, b, c -space passing through (2, 2, 2). By analogy with our codimension-2 flip bifurcation investigation of (14), it is easy to see that for $a = 2 + \mu_1$, $b = 2 + \mu_2$ and $c = 2 + \mu_3$ with μ_1, μ_2, $\mu_3 \geq 0$ sufficiently small, we have the following flip bifurcation properties: There are four stable 2-cycles; namely

$$\{(a + \phi^{(+)}(\sqrt{\mu_1}),\ b + \phi^{(+)}(\sqrt{\mu_2}),\ c + \phi^{(+)}(\sqrt{\mu_3})),$$
$$(a + \phi^{(-)}(\sqrt{\mu_1}),\ b + \phi^{(-)}(\sqrt{\mu_2}),\ c + \phi^{(-)}(\sqrt{\mu_3}))\},$$
$$\{(a + \phi^{(+)}(\sqrt{\mu_1}),\ b + \phi^{(+)}(\sqrt{\mu_2}),\ c + \phi^{(-)}(\sqrt{\mu_3})),$$
$$(a + \phi^{(-)}(\sqrt{\mu_1}),\ b + \phi^{(-)}(\sqrt{\mu_2}),\ c + \phi^{(+)}(\sqrt{\mu_3}))\},$$
$$\{(a + \phi^{(+)}(\sqrt{\mu_1}),\ b + \phi^{(-)}(\sqrt{\mu_2}),\ c + \phi^{(+)}(\sqrt{\mu_3})),$$
$$(a + \phi^{(-)}(\sqrt{\mu_1}),\ b + \phi^{(+)}(\sqrt{\mu_2}),\ c + \phi^{(-)}(\sqrt{\mu_3}))\}$$

and

$$\{(a + \phi^{(+)}(\sqrt{\mu_1}),\ b + \phi^{(-)}(\sqrt{\mu_2}),\ c + \phi^{(-)}(\sqrt{\mu_3})),$$
$$(a + \phi^{(-)}(\sqrt{\mu_1}),\ b + \phi^{(+)}(\sqrt{\mu_2}),\ c + \phi^{(+)}(\sqrt{\mu_3}))\}$$

Moreover, there are ten unstable 2-cycles, which are the fixed point $(a,\ b,\ c)$ and the nontrivial 2-cycles

$$\{(a + \phi^{(+)}(\sqrt{\mu_1}),\ b,\ c),\ (a + \phi^{(-)}(\sqrt{\mu_1}),\ b,\ c)\}$$
$$\{(a,\ b + \phi^{(+)}(\sqrt{\mu_2}),\ c),\ (a,\ b + \phi^{(-)}(\sqrt{\mu_2}),\ c)\}$$
$$\{(a,\ b,\ c + \phi^{(+)}(\sqrt{\mu_3})),\ (a,\ b,\ c + \phi^{(-)}(\sqrt{\mu_3}))\}$$

$$\{(a+\phi^{(+)}(\sqrt{\mu_1}),\ b+\phi^{(+)}(\sqrt{\mu_2}),\ c),\ (a+\phi^{(-)}(\sqrt{\mu_1}),\ b+\phi^{(-)}(\sqrt{\mu_2}),\ c)\}$$

$$\{(a+\phi^{(+)}(\sqrt{\mu_1}),\ b+\phi^{(-)}(\sqrt{\mu_2}),\ c),\ (a+\phi^{(-)}(\sqrt{\mu_1}),\ b+\phi^{(+)}(\sqrt{\mu_1}),\ c)\}$$

$$\{(a+\phi^{(+)}(\sqrt{\mu_1}),\ b,\ c+\phi^{(+)}(\sqrt{\mu_3})),\ (a+\phi^{(-)}(\sqrt{\mu_1}),\ b,\ c+\phi^{(-)}(\sqrt{\mu_3}))\}$$

$$\{(a+\phi^{(+)}(\sqrt{\mu_1}),\ b,\ c+\phi^{(-)}(\sqrt{\mu_3})),\ (a+\phi^{(-)}(\sqrt{\mu_1}),\ b,\ c+\phi^{(+)}(\sqrt{\mu_3}))\}$$

$$\{(a,\ b+\phi^{(+)}(\sqrt{\mu_2}),\ c+\phi^{(+)}(\sqrt{\mu_3})),\ (a,\ b+\phi^{(-)}(\sqrt{\mu_2}),\ c+\phi^{(-)}(\sqrt{\mu_3}))\}$$

$$\{(a,\ b+\phi^{(+)}(\sqrt{\mu_2}),\ c+\phi^{(-)}(\sqrt{\mu_3})),\ (a,\ b+\phi^{(-)}(\sqrt{\mu_2}),\ c+\phi^{(+)}(\sqrt{\mu_3}))\}$$

In view of our analysis of codimension-2 flip bifurcations for our hierarchical map, it should come as no surprise that the qualitative behavior of the general case is the same as the uncoupled case. More precisely, we have the following result that can be proved readily, but with many routine detailed calculations, which we leave to the reader.

Theorem 6.4.1. *Suppose that all three of the eigenvalues of (6.23) are equal to -1 at a fixed point $\hat{x}$ of T for a particular set of parameter values $(a,\ b,\ c) = (a_0,\ b_0,\ c_0)$ and consider $(a,\ b,\ c) = (a_0,\ b_0,\ c_0) + (\mu_1,\ \mu_2,\ \mu_3)$ for sufficiently small $\mu_1,\ \mu_2,\ \mu_3 \geq 0$, defining $\hat{x} = \hat{x}(a,b,c)$ and $x_* = \hat{x}(a,\ b,\ c) + (y_1,\ y_2,\ y_3)$. Then for $\mu_1,\ \mu_2,\ \mu_3 > 0$ sufficiently small, $T^2(x_*) = x_*$ has 27 solutions comprising a total of thirteen(nontrivial) two-cycles of T near $\hat{x}(a_0,\ b_0,\ c_0)$ and the fixed point. These 2-cycles consist of four stable 2-cycles, and nine unstable 2-cycles; while the fixed point $\hat{x}$ is unstable. All of these 2-cycles depend analytically on $(\sqrt{\mu_1},\ \sqrt{\mu_2},\ \sqrt{\mu_2})$ for sufficiently small $\mu_1,\ \mu_2,\ \mu_3 \geq 0$, and shrink to $\hat{X}(a_0,\ b_0,\ c_0)$ as $\sqrt{\mu_1}+\sqrt{\mu_2}+\sqrt{\mu_3} \downarrow 0$.*

CHAPTER 7

CHAOTIC DYNAMICS

Perhaps the most interesting behavior that one may observe in population dynamics is transition to chaotic regimes, possibly including strange chaotic attractors. From an ecologist's point of view, chaos plays an important role in predicting (or more accurately not being able to make long-time predictions about) the growth of plants in an ecosystem. If chaotic dynamics occurs, the behavior of the species can, besides being quite unpredictable to the point of appearing stochastic, be extremely complex and especially interesting. It appears from our simulations that our 3-dimensional all climax discrete hierarchical model can exhibit chaotic dynamics, as shown in Figure 7.1 for the case where

$$x_1(n+1) = x_1(n)(x_1(n))e^{2.7-x_1}$$
$$x_2(n+1) = x_2(n)(x_1(n)+x_2(n))e^{2.8-x_1(n)-x_2(n)}$$
$$x_3(n+1) = x_3(n)(x_1(n)+x_2(n)+x_3(n))e^{3-x_1(n)-x_2(n)-x_3(n)}$$

We have already proved that the one-dimensional pioneer case has a 3-cycle, which induces chaos in our hierarchical system if it is the first coordinate. As a matter of fact, it is not difficult to adapt our flip bifurcation proofs in the preceding section to show that essentially one-dimensional chaos in any component (pioneer or climax) induces chaos in the whole hierarchical system. The bifurcation diagrams for the one-dimensional pioneer case in Figure 7.2 and Figure 7.3 suggests the existence of chaos. Lyapunov exponent computations results in Figure 7.4 support and illustrate our conclusion about chaos. Note from Figure 7.2 and Figure 7.3 that the bifurcation diagram in both the pioneer and climax cases appears to collapse to zero beyond a certain parameter value . In the climax case, zero is superstable, but in the pioneer

case where zero is unstable, it may be that there is a small scale strange attractor for sufficiently large parameter values.

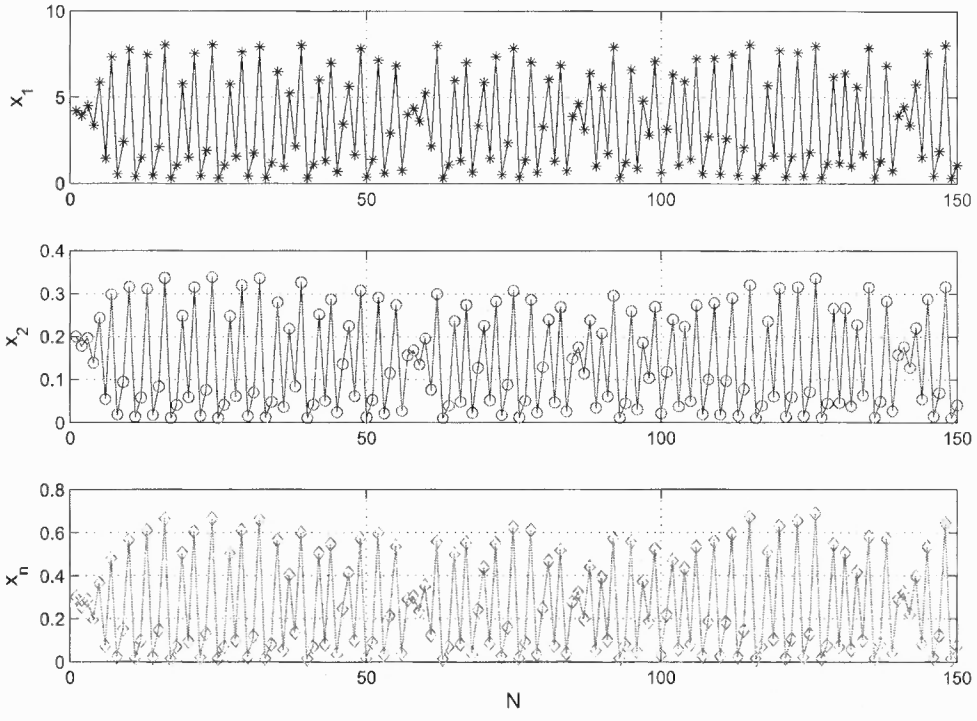

Figure 7.1 Chaotic behavior for the all climax discrete hierarchical case with $a = 2.7$, $b = 2.8$, $c = 3.0$. The interspecies and intraspecies interaction coefficients are 1.

Figures 7.2, 7.3 show the behavior of a pioneer species for a range of values of a. It appears that one has chaos in the limit of the period doubling cascade. The graphs shown in Figures 7.2 and 7.3 as a result of numerical simulation supports our view of a chaotic period-doubling limit. Initially as a varies from 0 to 2 we have a single stable fixed point solution. But as we exceed 1.985, the single stable solution bifurcates into a stable 2-cycle via period-doubling bifurcation. This two-cycle further bifurcates into a stable 4-cycle and these period-doubling bifurcations continue with increasing a, generating a period-doubling cascade that reaches a limit at $a = 2.69$. At

$a = 3.105$ we have a period-3 window showing the existence of chaos for a single species owing to the work of Sharkovski [43] and Li and Yorke [29]. Beyond $a = 8.575$ it looks like the bifurcation diagram degenerates to the line at zero - but this may be misleading as a smaller scale image might reveal that this is just a thin, chaotic strip comprising a strange attractor near the origin. This behavior indicated by our simulations remains to be proved - a problem we shall explore in a future study.

In Figure 7.4 we have plotted Lyapunov exponents λ for various values of a for the same species. Positive λ indicates chaotic orbits.

For the climax case, we have analogous period-doubling cascades leading to chaos. However, in this case the diagram collapses to the superstable attractor at the origin for sufficiently small parameter values as compared to the pioneer case. We note here that such bifurcation or chaotic phenomena exhibited by any component of the hierarchical system - be it pioneer or climax - is actually induced in the entire dynamical system.

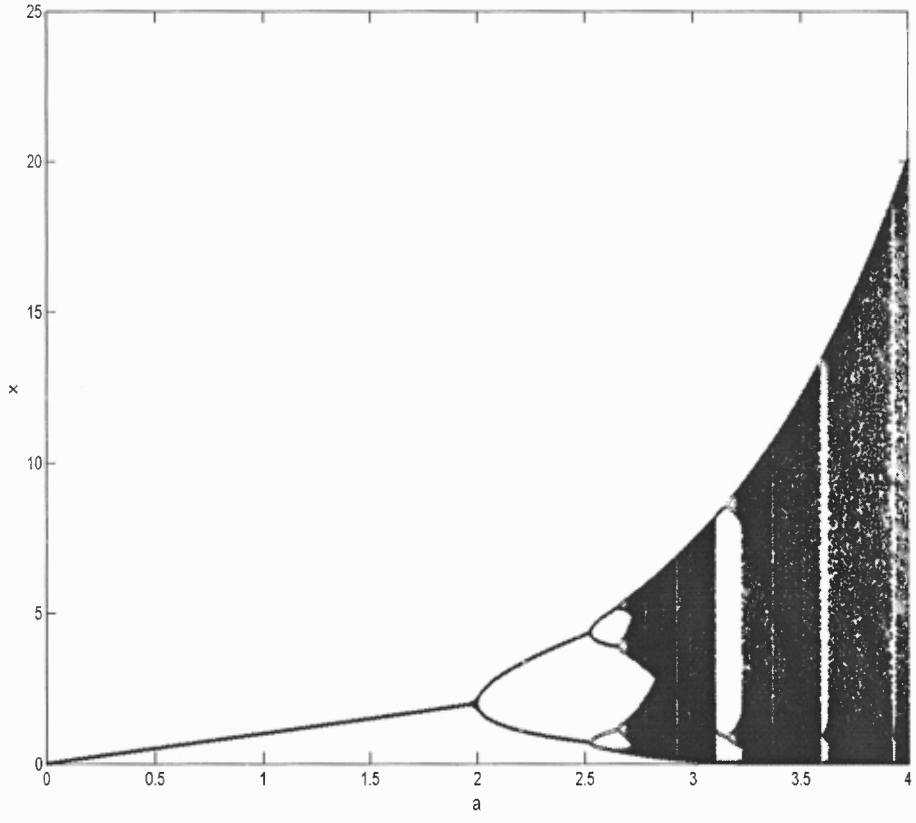

Figure 7.2 Bifurcation diagram for a pioneer species. Here the parameter a varies from 0-4.

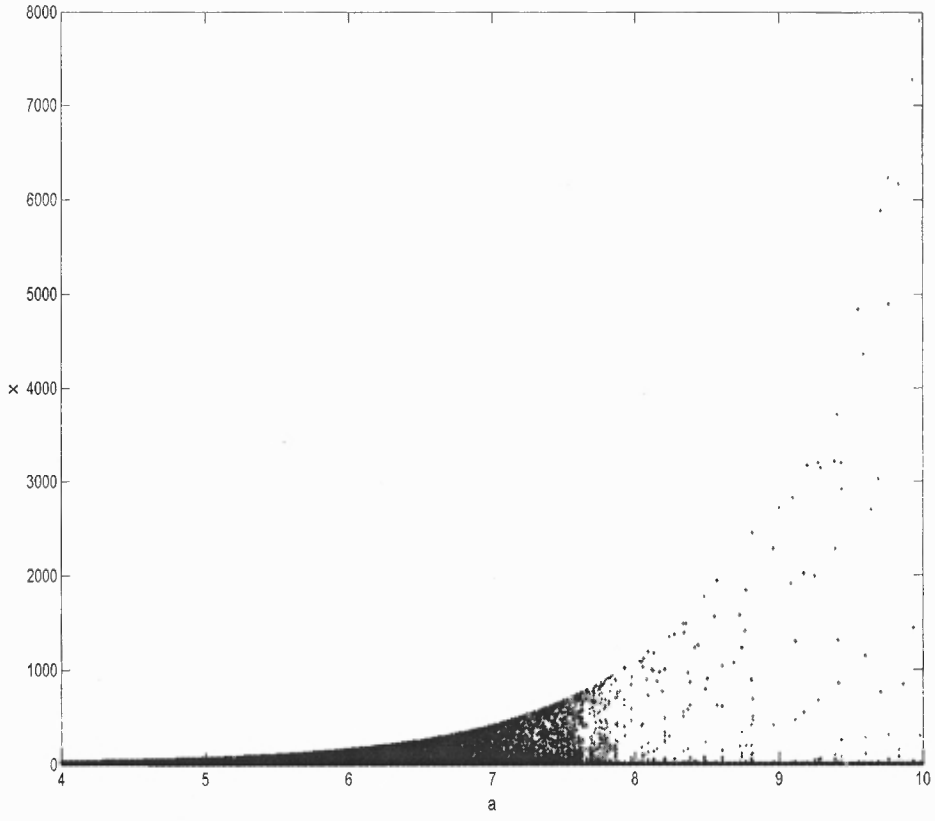

Figure 7.3 Bifurcation diagram for a pioneer species. Here the parameter a varies from 4-10.

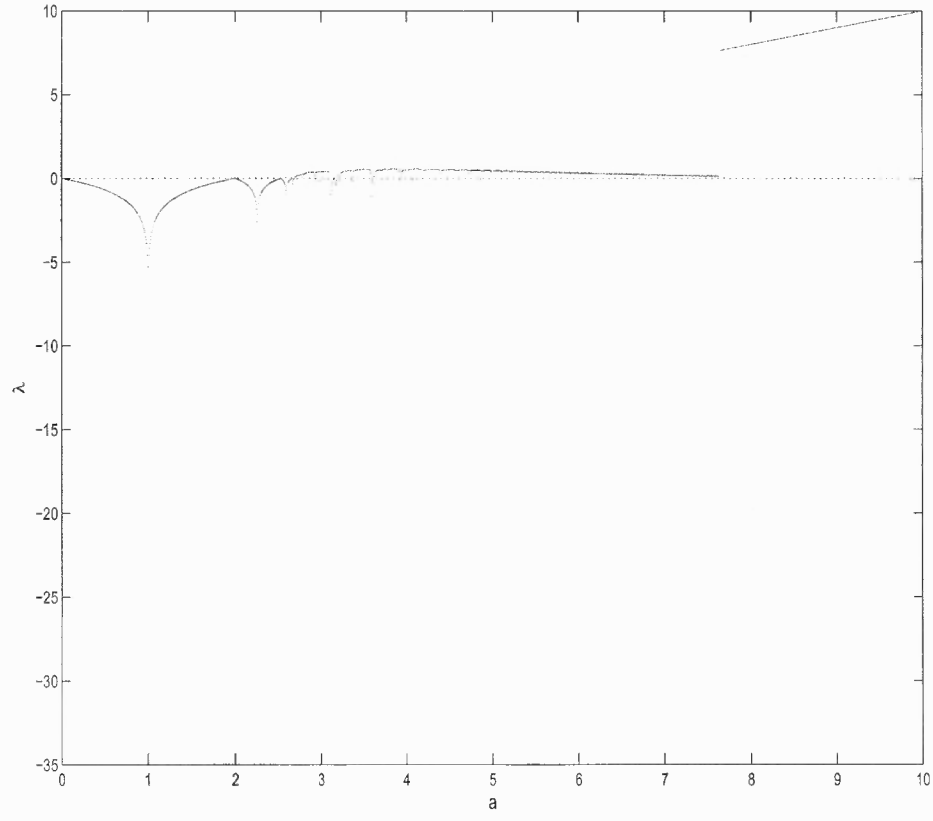

Figure 7.4 Lyapunov exponents for a pioneer species.

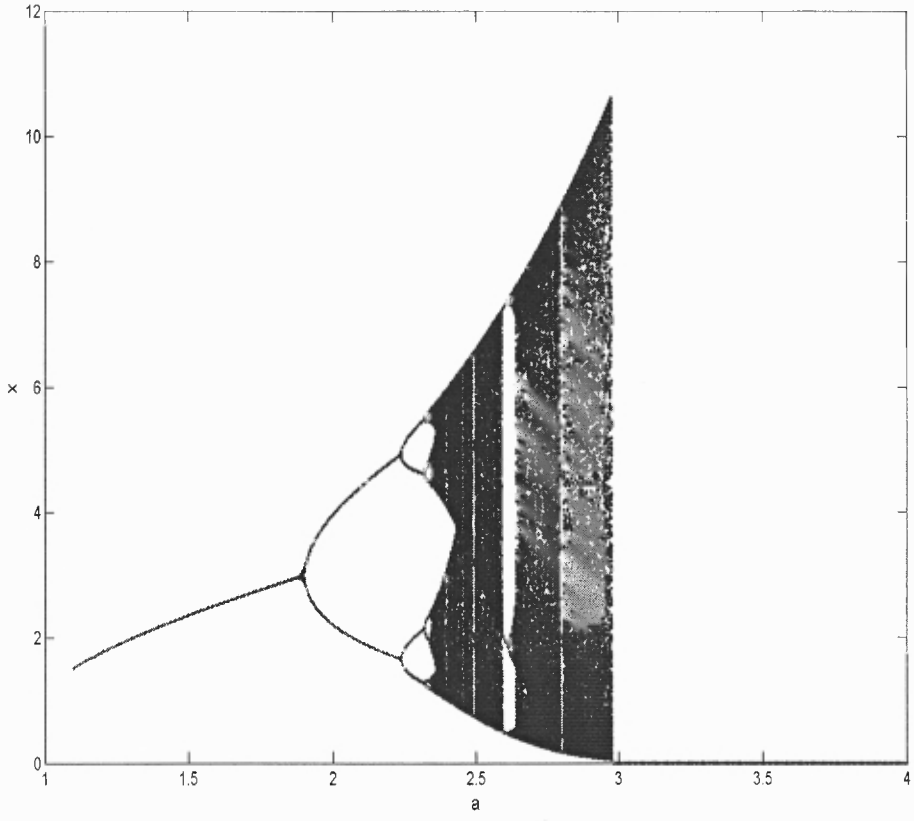

Figure 7.5 Bifurcation diagram for a climax species. Here the parameter a varies from 1.1-4.

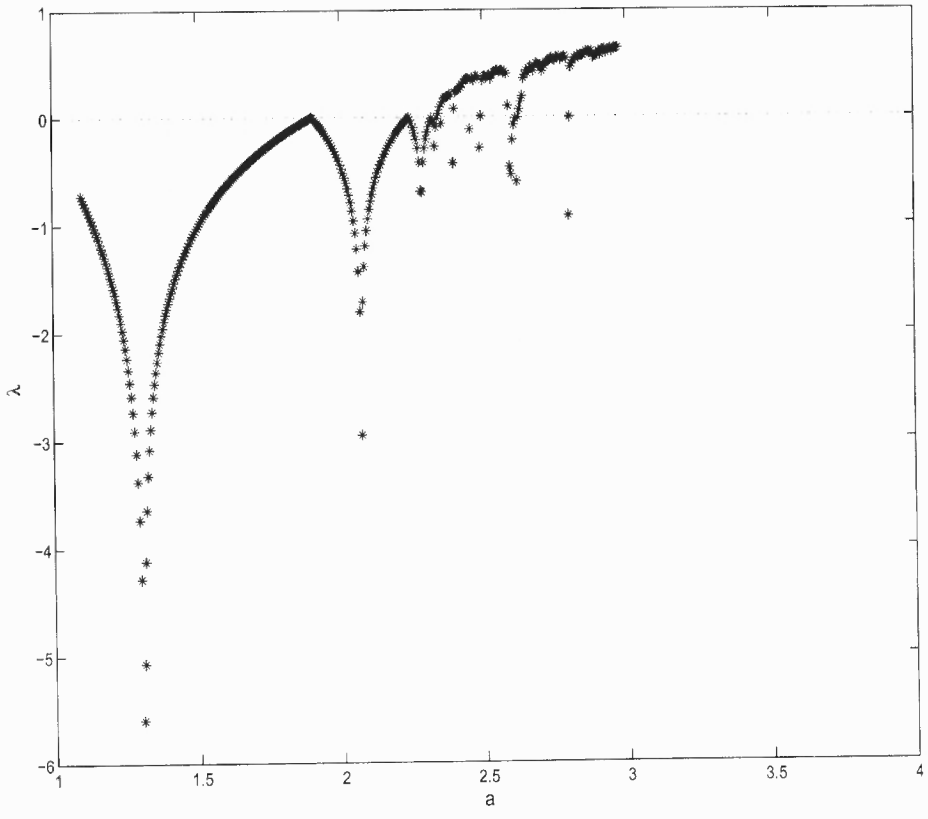

Figure 7.6 Lyapunov exponents for a climax species.

7.1 Existence of Chaos on a Cantor Set

Consider the one-dimensional climax species

$$x_1(n+1) = x_1(n)c_{11}x_1(n)e^{a-c_{11}x_1(n)} \tag{7.1}$$

We will do the analysis for $c_{11} = 1$, (but the same procedure can be applied when $c_{11} \neq 1$ with some obvious changes) so the above equation reduces to

$$x_1(n+1) = x_1(n)^2 e^{a-x_1(n)} \tag{7.2}$$

Now consider $f_a(x) = x^2 e^{a-x}$. Numerical experiments indicate that we can apply the standard Cantor set argument to prove existence of chaos when $a \geq 2.98$. So we will now focus our attention on

$$f_a(x) = x^2 e^{2.98-x} \tag{7.3}$$

The fixed points of f_a are 0, 0.0536 and 4.4795. An $x \in I = [0.0536,\ 10.6436]$ has two types of orbits: one which directly or eventually goes to origin (extinction or saturation of population leading to extinction) and a second which does not converge to the origin (flourishing). We are interested in the second case. So, we will remove all the subintervals from I which give rise to orbits converging to the origin and then observe the behavior of (7.3) on the remainder of I

Let us denote the set of all points in I whose iterates do not converge to the origin by Λ. We clearly have the subinterval $I_0 = (1.54,\ 2.55)$ whose points ultimately go to the origin. Next we have two more subintervals: $I_1^{(-)} = (0.32,\ 0.45)$ on the left of I_0 and $I_1^{(+)} = (5.42,\ 6.19)$ on the right of I_0. They represent $f^{-1}(I_0)$ the preimage of I_0. So the points in $I_1^{(-)}$, $I_1^{(+)}$ are first mapped to I_0 and then they go to the origin. We will remove these three subintervals from I. Now we repeat this procedure again, *i.e.* to find the preimage of $I_1^{(-)}$ which is $I_2^{(-)} = (0.13,\ 0.16) \cup (0.77,\ 0.86)$ and of $I_1^{(+)}$ which is $I_2^{(+)} = (3.85,\ 4.12) \cup (7.91,\ 8.36)$. At any stage k of this process, we

find 2^k subintervals whose forward iterates under f_a converge to the origin, and are to be removed from I.

This process of removal generates a 2-component Cantor set defined as

$$\Lambda = I \backslash (I_0 \cup (\cup_{k=1}^{\infty} I_k^{(\pm)}))$$

It is clear from the construction that $f_a(\Lambda) \subset \Lambda$, so this Cantor set is invariant.

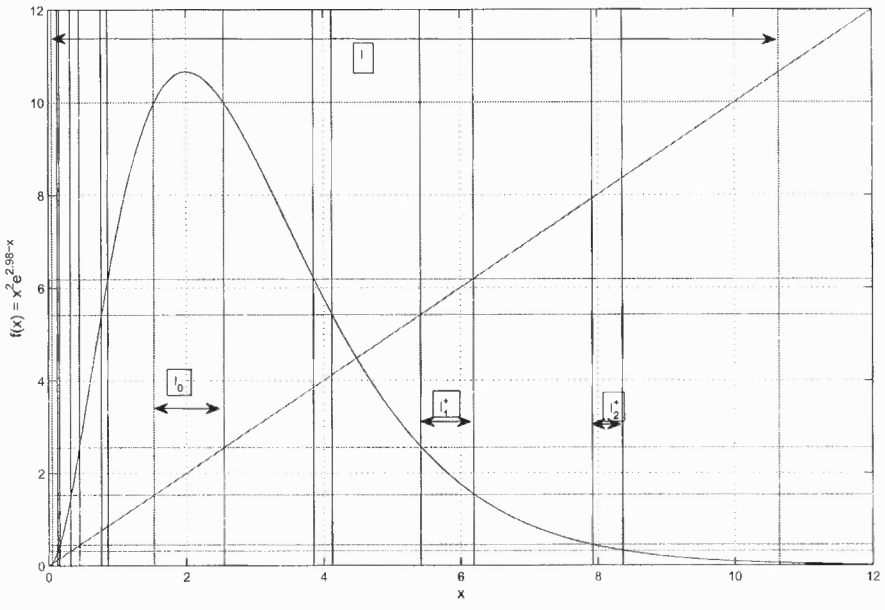

Figure 7.7 The formation of the Cantor set.

Each $x \in \Lambda$ can be identified with a binary sequence as follows:

$$x \leftrightarrow .a_0 a_1 a_2 \ldots$$

where,

$$a_j = \begin{cases} 0 & \text{if } f_a^j(x) \in J_0; \\ 1 & \text{if } f_a^j(x) \in J_1, \end{cases}$$

with $J_0 = [0.0536, 1.54)$ and $J_1 = (2.55, 10.6436]$. The fixed points 0.0536 and 4.4795 will naturally belong to J_0 and J_1, respectively, since the iterates of these points are fixed which means their iterates remain in their corresponding intervals. In terms of the identification (homeomorphism), the positive fixed points are identified with the points .0000... and .1111...

The restriction $f_a|_\Lambda$ is, by a standard argument (see [1, 4, 14]) that follows right from its definition, topologically conjugate to the shift map $\sigma : S \to S$, defined in the space of binary sequences of the form $a_0a_1a_2\ldots$ as

$$\sigma(a_0a_1a_2\ldots) = a_1a_2a_3\ldots$$

Therefore, $f_a|_\Lambda$ is chaotic and has such features as periodic orbits of all periods and a dense orbit.

7.2 Geometric Proof of Chaos Based on Horseshoe Behavior

Demonstrating that a map behaves like a Smale horseshoe in some region is another method that can be used to show the existence of chaos. When a map acts on a geometric figure and shows contraction, expansion and folding of the resulting figure onto the original one to form two or more components in the manner of Smale's construction, then the horseshoe argument can be applied to the map to prove chaos. In Figures 7.8-7.10 some numerical simulations are shown that indicate contraction, expansion and folding occurs in three-dimensional horseshoe-like fashion for the 3-dimensional pioneer-climax hierarchical system.

In Figure 7.8(a) we first plotted the tetrahedron $ABCD$ with $A(0.05, 1.5, 3)$, $B(0.05, 3, 1.5)$, $C(0.05, 1.5, 1.5)$, $D(10.7, 1.2, 1.2)$ and then studied its image under the following

map:

$$
\begin{aligned}
x_1(n+1) &= x_1(n)(x_1(n))e^{3-x_1} \\
x_2(n+1) &= x_2(n)(0.01x_1(n)+x_2(n))e^{1.3-0.01x_1(n)-x_2(n)} \\
x_3(n+1) &= x_3(n)(0.01x_1(n)+0.01x_2(n)+x_3(n))e^{1.28-0.01x_1(n)-0.01x_2(n)-x_3(n)}
\end{aligned}
\tag{7.4}
$$

The resulting figure presented in Figure 7.8(b) was superimposed on the original tetrahedron to show contraction, expansion and folding behavior together with two-component intersection shown in Figure 7.9. With this, we can essentially repeat the standard horseshoe argument to show that there is an invariant Cantor set on which (7.4) behaves like a shift map, which implies that (7.4) is chaotic.

It is important to note that the necessary behavior of the intersection of the given region with its image under the map (7.4) can be readily verified in a direct - but long and tedious analytical fashion. Consequently, the "picture proof" in Figures 7.8-7.10 can be rather routinely transformed into actual three-dimensional proofs of horseshoe behavior that generates chaos.

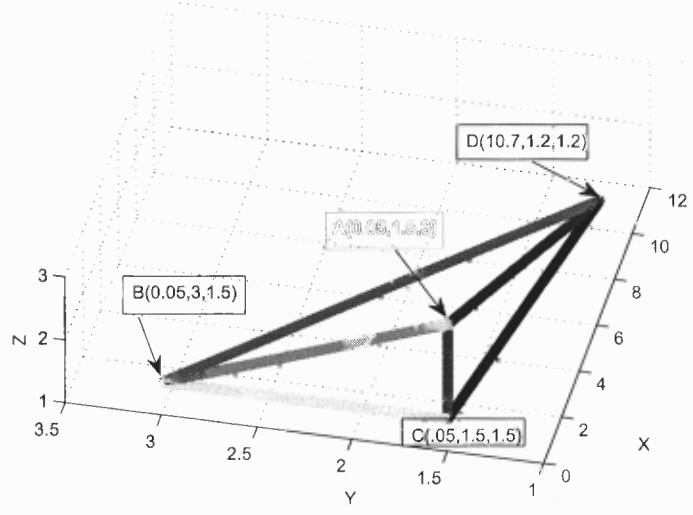

(a) Tetrahedron $ABCD$ with A(0.05,1.5,3), B(0.05,3.1.5), C(0.05,1.5,1.5), D(10.7,1.2,1.2) which is acted upon by (7.4).

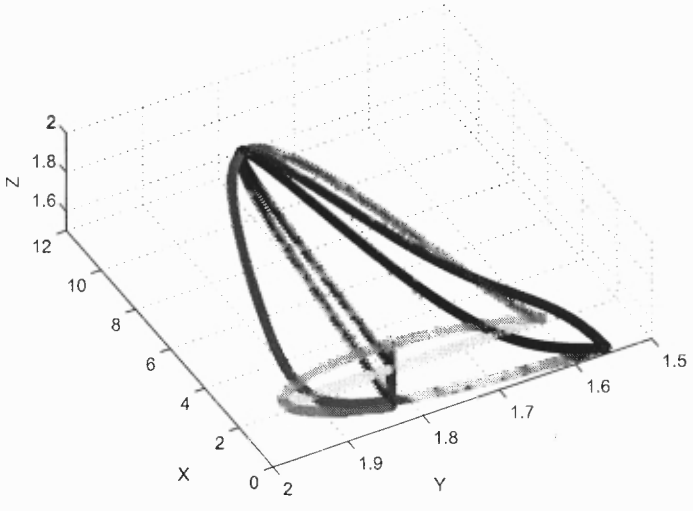

(b) Transformed tetrahedron under the action of (7.4).

Figure 7.8 Horseshoe behavior observed in the all climax hierarchical system.

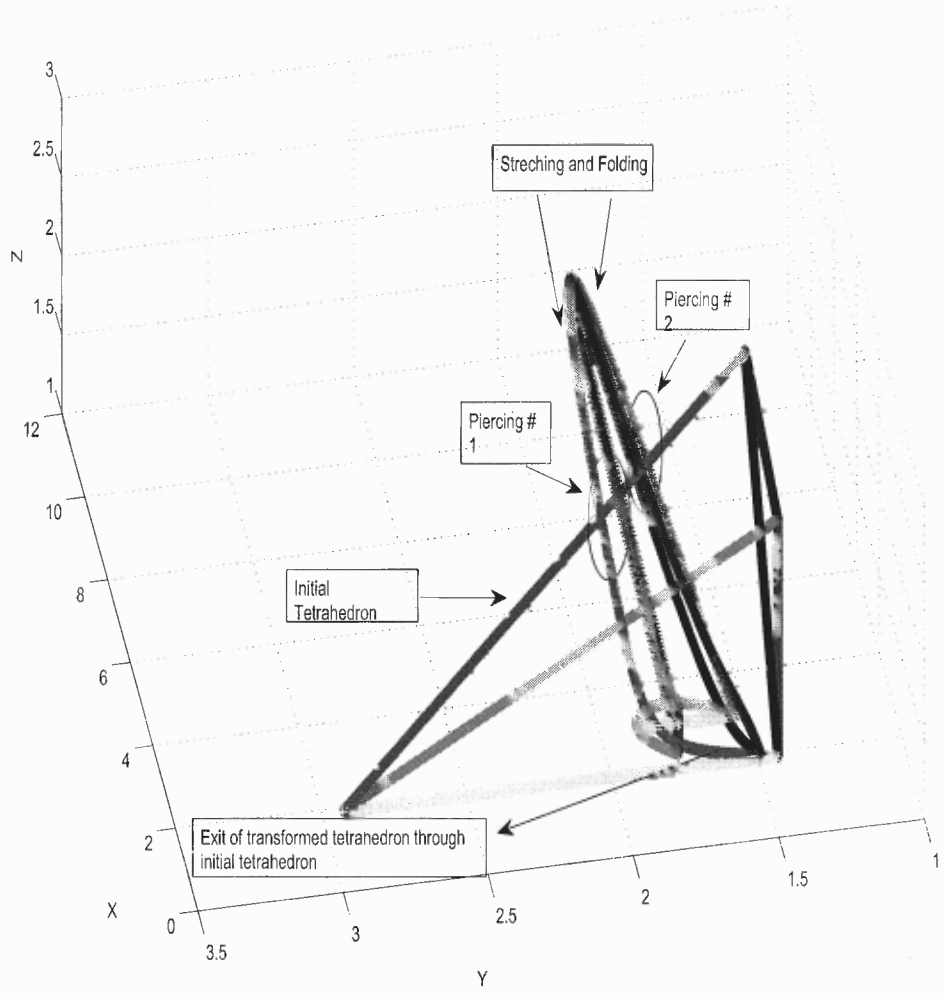

Figure 7.9 The transformed tetrahedron superimposed on the initial tetrahedron.

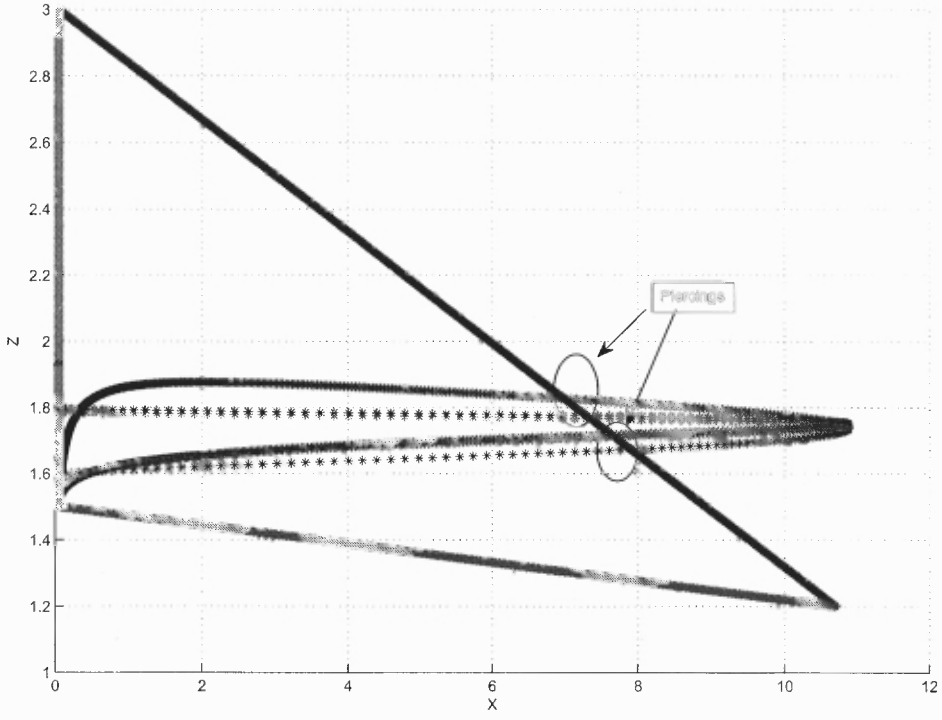

Figure 7.10 The X-Z view of the the intersection of the transformed tetrahedron with the initial tetrahedron.

CHAPTER 8

CONCLUSIONS AND FUTURE RESEARCH

In this chapter we conclude this dissertation by summarizing various results obtained in the course of our research, with a special emphasis on the discoveries and innovations that represent advances in the state-of-the-art of dynamical analysis of population models.

We began this dissertation by citing some of the famous and widely used models of population dynamics of various species. Then we formulated a discrete dynamical model general enough to subsume most of the models in the literature. Unfortunately, the general nature of our model precluded an extensive dynamical analysis, but we were able to prove some theorems on the existence of fixed (equilibrium) points. We hope in future to delve more deeply into the dynamics of certain interesting special cases of our general system, but we decided to concentrate for the rest of our dissertation research on rather specific (hierarchical pioneer-climax) models used to predict the behavior of ecological populations.

In Chapter 3, we introduced the forestry terms pioneer species and climax species both from ecological and mathematical modeling sense. The discrete dynamical models were taken to be hierarchical since it has been found that such models produce dynamics closer to that observed in real-world behavior of pioneer and climax species. Then for concreteness, we restricted our attention to hierarchical models with three distinct species. Fixed points were found for 3-dimensional hierarchical model for some combinations of pioneer and climax in Chapter 4. A local stability analysis of the fixed points was then performed. We ended the chapter by proving a lemma which gave conditions on the intrinsic parameters a, b, and c as to when $(0,0,0)$ is an attractor or a repeller for the 3-dimensional all pioneer hierarchical model. Some of

the main contributions of this dissertation are in Chapters 5 and 6, where we analyzed the periodic behavior and bifurcations, respectively, of our 3-dimensional hierarchical system. We began chapter 5 by deriving sufficient conditions for the existence of period-2 orbits for 3-dimensional all pioneer hierarchical model. Further conditions for stable period-2 orbits were obtained using symbolic mathematics in MATLAB. Several $n-$ cycles for $n > 1$ were also identified in our hierarchical model. In particular, we proved the existence of a stable 3-cycle for a certain range of parameters for an all pioneer model, and indicated how a similar result can be proved for any combination of three species. In light of our observation that periodic, bifurcation or chaotic behavior in any component induces this behavior in the whole hierarchical system, the existence of the three cycle indicated that the system might exhibit chaos in virtue of the work of Li and Yorke [29].

In Chapter 6, we first noted by a simple computation that our 3-dimensional hierarchical model cannot exhibit a Hopf Bifurcation. As a matter of fact, the hierarchical nature of the model precludes Hopf bifurcations. However, the model can exhibit a very rich flip (period-doubling) bifurcation structure, which can produce the birth of cycles from fixed points. These cycles can be of period 2, 4 or 8 depending on the codimension of the flip bifurcation. This type of behavior appears not to have been discovered in the literature.

Finally in Chapter 7, we analyzed chaotic behavior in the 3-dimensional, hierarchical pioneer-climax model. First, we observed what appeared to be chaotic regimes for certain parameter ranges in several numerical simulations. We next noted from bifurcation diagrams for a single pioneer and climax species that there were strong indications of the typical period-doubling route to chaos. Then we used a rather standard two-component Cantor set construction to show that a single climax species has, for a certain range of its parameters, an (unstable) invariant set on which the dynamical system is conjugate to a shift map, and so is chaotic. This result,

coupled with our proof that a single pioneer species has a stable 3-cycle for a range of parameter values, leads to the conclusion that if the first component of our hierarchical model has these properties, the entire system is chaotic. Actually, it is not too far a stretch to prove that what is essentially 1-dimensional chaos in any component, induces chaotic regimes in the whole hierarchical system. In fact a proof of this and some related results is something that we shall tackle in our future research. The results on chaos were underscored by graphing the Lyapunov exponents for the one-species pioneer and climax cases, which yielded a preponderance of positive values (implying chaos) for large enough parameter values.

One of our goals in studying chaotic dynamics for our hierarchical system was to obtain definitive evidence of strange attractors for some parameters ranges. However, the best that we were able to do at this juncture was to find an intriguing clue: We noted from our simulations of a single pioneer species that the bifurcation diagram (which records only stable states) appears to collapse to zero for sufficiently large values of its main (exponential) parameter. But for these parameter values, the origin is actually quite a strong repeller. This suggests that there may be a strange attractor very close to the origin, and indicates that hierarchical systems containing at least one pioneer component may be exhibiting interesting stable chaotic behavior at very small scales - perhaps at scales too small to have registered in certain experimental studies of pioneer-climax systems. This is definitely something we are planning to investigate in future research, perhaps in collaboration with ecologists who might be able to confirm the existence of such small scale strange attractors by using the proper focus in their field work. Such collaborations with ecologists may be indispensable to our future research in this vein, since the available data at this juncture is not well suited to testing the efficacy of dynamical models.

Our final proof of the existence of chaotic regimes entailed a demonstration that the map associated to our 3-dimensional hierarchical system behaved like a

3-dimensional Smale horseshoe map on a properly chosen initial region, taken to be a tetrahedron. We were content with what amounted to graphical "picture-proofs" of these results since the analysis, although straightforward, is quite lengthy. The details of such an analysis shall be provided in our future research.

REFERENCES

[1] T. Alligood, K. Sauer and J. Yorke. *Chaos: An Introduction to Dynamical Systems.* Springer-Verlag, New York, 1997.

[2] T M. Apostol. *Mathematical Analysis.* Addison Wesley Longman, Inc., 1974.

[3] D. K. Arrowsmith and C. M. Place. *An Introduction to Dynamical Systems.* Cambridge University Press, Cambridge, 1990.

[4] D. K. Arrowsmith and C. M. Place. *Dynamical Systems: Differential Equations, Maps and Chaotic Behaviour.* Chapman and Hall, London, 1992.

[5] J. Best, C. Castillo-Chavez, and A.-A. Yakubu. Hierarchical competition in discrete time models with dispersal. *Fields Institute Communications*, 36:59-86, 2004.

[6] R. M. Corless, G. H. Gonnet, D. E. G. Hare, D. J. Jeffrey, and D. E. Knuth. On the Lambert W function. *Adv. Computational Maths*, 5:329-359, 1996.

[7] J. M. Cushing. The LPA Model. *Fields Institute Communications*, 43:29-55, 2004.

[8] J. M. Cushing, S. Levarge, N. Chitnis, and S. M. Henson. Some discrete competition models and the competitive exclusion principle. *Journal of Difference Equations and Applications*, (13-15):1139-1151, 2004.

[9] R. Devaney. *An Introduction to Chaotic Dynamical Systems.* Addison-Wesley, Redwood City, 1989.

[10] A. Diller. *LaTeX: Line by Line: Tips and Techniques for Document Processing.* Wiley, New York, 1999.

[11] J. E. Franke and A-A Yakubu. Exclusion principles for density-dependent discrete pioneer-climax models. *Journal of Mathematical Analysis and Applications*, 187:1019-1046, 1994.

[12] J. E. Franke and A-A. Yakubu. Pioneer exclusion in a one-hump discrete pioneer-climax competitive system. *J. Math. Biol.*, 32:771-787, 1994.

[13] M. Goossens, F. Mittelbach, and A. Samarin. *The LaTeX Companion.* Addison Wesley, New York, 1994.

[14] J Guckenheimer and P. Holmes. *Nonlinear Oscillations, Dynamical Systems and Bifurcations of Vector Fields.* Springer-Verlag, New York, 1983.

[15] J. Hale and H. Kocak. *Dynamics and Bifurcations.* Springer-Verlag, New York, 1991.

[16] I. Hanski. Single-spcies metapopulation dynamics-concepts, models and observations. *Biol. J. Linn. Soc.*, 42:17-38, 1991.

[17] M. E. Hanski, I. A. and Gilpin. *Metapopulation Biology: ecology, genetics, and evolution.* Academic Press Ltd., San Diego, California, 1997.

[18] M. P. Hassell and M. N. Comins. Discrete time models for two-species competition. *Theoret. Population Biol.*, 9:202-221, 1976.

[19] M W. Hirsch. *Differential Topology.* Springer, New York, 1980.

[20] M. W. Hirsch, S. Smale, and R. L. Devaney. *Differential Equations, Dynamical Systems, And An Introduction To Chaos.* Elsevier Academic Press, New York, 2004.

[21] A. V. Holden. *Chaos.* Princeton University Press, Princeton, N.J., 1986.

[22] G. Jegan, G. Ramesh, and K. Muthuchelian. Resprouting of pioneer and climax species in the Pachakumachi Hills, Cumbum Valley, Western Ghats, India. *Ethnobotanical Leaflets*, 12:343-347, 2008.

[23] A. Kendall. *An Introduction to Numerical Analysis.* Wiley, New York, 1989.

[24] W. Krabs. A general predator-prey model. *Mathematical and Computer Modeling of Dynamical Systems*, 9:387-401, 2003.

[25] M. V. Kuijk. *Forest regeneration and restoration in Vietnam.* PhD thesis, Utrecht University, 2008.

[26] S. A. Levin. Dispersion and population interactions. *Amer. Naturalist*, 108:207-228, 1974.

[27] S. A. Levin. The problem of pattern and scale in ecology. *Ecology*, 73:1943-1967, 1992.

[28] R. Levins. Some demograhic and genetic consequences of environmental heterogeneity for biological control. *Bull. Entomol. Soc. Am.*, 15:237-240, 1969.

[29] Y. T. Li and J. A. Yorke. Period three implies chaos. *Am. Math. Month.*, 82:985-992, 1975.

[30] R. May. Simple mathematical models with very complicated dynamics. *Nature*, 261:459-467, 1976.

[31] A. Medio and M. Lines. *Nonlinear Dynamics: A Primer.* Cambridge University Press, New York, 2001.

[32] F. C. Moon. *Chaotic and Fractal Dynamics.* John Wiley and Sons, Inc., New York, 1992.

[33] L. Perko. *Differential Equations and Dynamical Systems.* Springer, New York, 1996.

[34] D. Raaimakers, R. G. A. Boot, R. Dijkstra, S. Pot, and T. Pons. Photosynthetic rates in relation to leaf phosphorus content in pioneer versus climax tropical rainforest trees. *Oecologia*, 102:120-125, 1995.

[35] D. Raaimakers' and H. Lambers. Response to phosphorus supply of tropical tree seedlings: a comparison between a pioneer species tapirira obtusa and a climax species lecythis corrugata. *Netv PhytoL*, 132:97-102, 1996.

[36] C. Robinson. *Dynamical Systems: Stability, Symbolic Dynamcis, and Chaos.* CRC Press, Inc, Boca Raton, 1995.

[37] J. F. Selgrade. Planting and harvesting for pioneer-climax models. *Rocky Mountain Journal of Mathematics*, 24:293-310, 1994.

[38] J. F. Selgrade and G. Namkoong. Stable periodic behavior in a pioneer-climax model. *Nat. Resour. Model*, 4:215-227, 1990.

[39] J. F. Selgrade and G. Namkoong. Population interactions with growth rates dependent on weighted densities. *Differential equation models in biology, epidemiology and ecology, Lecture Notes in Biomath*, 92:247-256, 1991.

[40] J. F. Selgrade and J. H. Roberds. Lumped-density population models of pioneer-climax type and stability analysis of Hopf bifurcations. *Mathematical Biosciences*, 135:1-21, 1996.

[41] J. F. Selgrade and J. H. Roberds. Period-doubling bifurcations for systems of difference equations and applications to models in population biology. *Nonlinear Analysis, Theory, Methods and Applications*, 29:185-199, 1997.

[42] J. F. Selgrade and J. H. Roberds. Reversing period-doubling bifurcations in models of population interactions using constant stocking or harvesting. *Canadian Applied Mathematics Quarterly*, 6:207-231, 1998.

[43] A. N. Sharkovsky. Co-existence of the cycles of a continuous mapping of the line into itself. *Ukranian Math. Z.*, 16:61-71, 1964.

[44] M. Silvestrini, I. F. M. Válio, and E. A. de. Mattos. Photosynthesis and carbon gain under contrasting light levels in seedlings of a pioneer and a climax tree from a Brazilian semideciduous tropical forest. *Rev. bras. Bot.*, 30:463-474, 2007.

[45] S. H. Strogatz. *Nonlinear Dynamics and Chaos.* Addison-Wesley Publishing Company, New York, 1994.

[46] S. Sumner. *Dynamical Systems Associated with Pioneer-Climax Models.* PhD thesis, North Carolina State University, 1992.

[47] S. Sumner. Hopf bifurcation in pioneer-climax competing species models. *Math. Biosci.*, 137:1-24, 1996.

[48] P. F. Verhulst. Recherches mathématiques sur la loi d'accroissement de la population. *Nouv. mm. de l'Academie Royale des Sci.*, 18:1-41, 1845.

[49] P. F. Verhulst. Deuxième mémoire sur la loi d'accroissement de la population. *Mém. de l'Academie Royale des Sci.*, 20:1-32, 1847.

[50] S. Wiggins. *Introduction to Applied Nonlinear Dynamical Systems and Chaos.* Springer, New York, 2003.